

# *Haloferax volcanii* Proteome Response to Deletion of a Rhomboid Protease Gene

Mariana I. Costa,<sup>†,‡</sup> Micaela Cerletti,<sup>†,‡</sup> Roberto A. Paggi,<sup>†</sup> Christian Trötschel,<sup>‡</sup> Rosana E. De Castro,<sup>†</sup> Ansgar Poetsch,<sup>\*,‡,§</sup> and María I. Giménez<sup>\*,†,§</sup>

<sup>†</sup>Instituto de Investigaciones Biológicas, Universidad Nacional de Mar del Plata (UNMDP), Consejo Nacional de Investigaciones Científicas y Técnicas (CONICET), Funes 3250 4to nivel, Mar del Plata, Buenos Aires 7600, Argentina

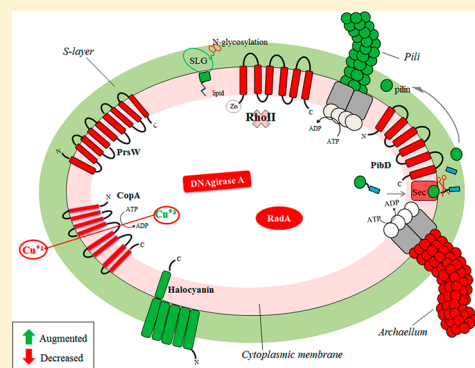
<sup>‡</sup>Plant Biochemistry, Faculty of Biology & Biotechnology, Ruhr University Bochum, 44801 Bochum, Germany

<sup>§</sup>School of Biomedical and Healthcare Sciences, Plymouth University, Plymouth PL4 8AA, United Kingdom

## Supporting Information

**ABSTRACT:** Rhomboids are conserved intramembrane serine proteases involved in cell signaling processes. Their role in prokaryotes is scarcely known and remains to be investigated in *Archaea*. We previously constructed a rhomboid homologue deletion mutant ( $\Delta\rho II$ ) in *Haloferax volcanii*, which showed reduced motility, increased novobiocin sensitivity, and an N-glycosylation defect. To address the impact of *rhoII* deletion on *H. volcanii* physiology, the proteomes of mutant and parental strains were compared by shotgun proteomics. A total of 1847 proteins were identified (45.8% of *H. volcanii* predicted proteome), from which 103 differed in amount. Additionally, the mutant strain evidenced 99 proteins with altered electrophoretic migration, which suggested differential post-translational processing/modification. Integral membrane proteins that evidenced variations in concentration, electrophoretic migration, or semitryptic cleavage in the mutant were considered as potential RhoII targets. These included a PrsW protease homologue (which was less stable in the mutant strain), a predicted halocyanin, and six integral membrane proteins potentially related to the mutant glycosylation (S-layer glycoprotein, Agl15) and cell adhesion/motility (flagellin1, HVO\_1153, PilA1, and PibD) defects. This study investigated for the first time the impact of a rhomboid protease on the whole proteome of an organism.

**KEYWORDS:** *Archaea*, *Haloferax volcanii*, rhomboid protease, shotgun proteomics, protease substrate



## 1. INTRODUCTION

Proteases cleave their protein/peptide substrates in an irreversible reaction, and through this activity they catalyze the fate and activity of other proteins. They control appropriate protein folding, localization, activation (or inactivation), and shedding from cell surfaces. Therefore, proteases control a wide range of important cellular functions including DNA replication, cell cycle progression, cell proliferation, cell–cell communication, differentiation, morphogenesis, neuronal outgrowth, homeostasis, wound healing, immunity, angiogenesis, and apoptosis.<sup>1,2</sup>

Intramembrane proteolysis, that is, the cleavage of peptide bonds within the plane of the cell membrane, is a mechanism conserved in the three domains of life. The genomes of every sequenced organism encode for intramembrane proteases (IMPs). These enzymes exert diverse biological functions and are considered as promising future drug targets.<sup>3</sup> Among IMPs, three major classes have been described, the GxGD-aspartyl proteases (eukaryal signal peptide peptidase SPP and presenilin families), rhomboids, and site 2 proteases (S2P).<sup>2</sup>

Rhomboid proteases (Rho) are widespread serine proteases, and to date they are the best understood IMPs.<sup>4</sup> In eukaryotic

organisms, they have been implicated in a variety of processes. In *Drosophila melanogaster*, a Rho activates epidermal growth factor receptors.<sup>5,6</sup> In mitochondria, the mammalian PARL rhomboid protease regulates cell homeostasis and has been implicated in the biology of diabetes and Parkinson's disease.<sup>7</sup> Rhomboids in parasites regulate adhesion to the host through processing of adhesins.<sup>8</sup> Recently, a role in fungal hypoxia adaptation through sterol regulatory element-binding protein activation has been reported.<sup>9</sup>

In prokaryotes, the role of Rho has been explored to a lesser extent. To date, the function of only one prokaryotic Rho, AarA from *Providencia stuartii*, has been elucidated. AarA cleaves an N-terminal extension of the twin arginine translocation (Tat) complex component TatA, allowing for the assembly of a functional Tat translocon and, hence, for the export of a still unidentified quorum sensing signal.<sup>10</sup> In addition, some bacterial rhomboid deletion mutants have been characterized even though no specific protease substrates were reported. A null mutant in the *Escherichia coli* rhomboid protease GlpG

**Received:** July 28, 2017

**Published:** January 5, 2018

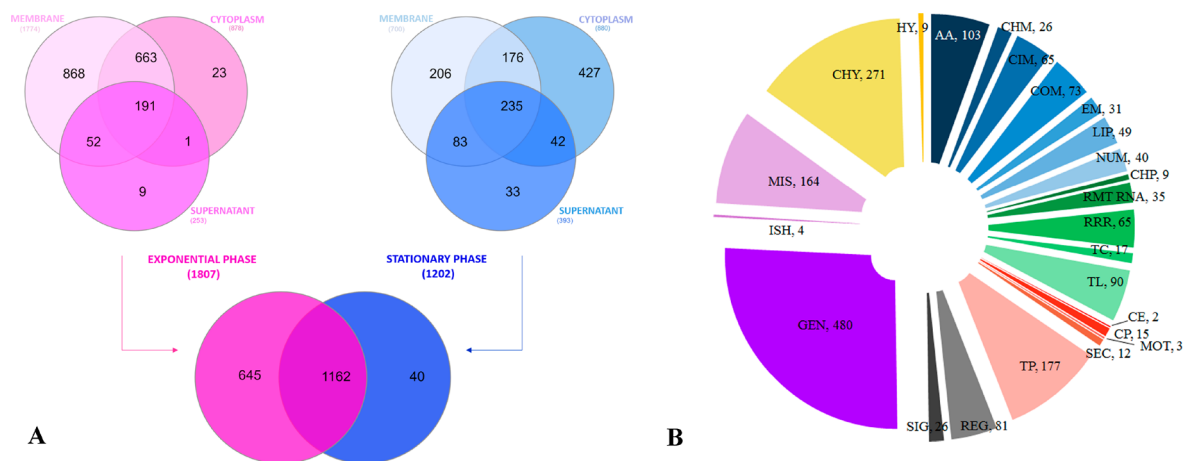


**Figure 1.** Total identified protein distribution in *H. volcanii* H26 and MIG1 strains. Protein detection was based on a minimum of two different peptides (in at least one biological replicate) with a minimal false discovery rate of  $q$ -value  $\leq 1\%$ . (A) Venn diagrams<sup>35</sup> showing the distribution of identified proteins in both strains and growth stages (center) and for each growth stage, the distribution of proteins according to cellular fraction (upper diagrams). (B) Functional categories corresponding to identified proteins, according to HaloLex Database. MET (metabolism, blue): AA amino acid metabolism, CHM carbohydrate metabolism, CIM central intermediary metabolism, COM coenzyme metabolism, EM energy metabolism, LIP lipid metabolism, NUM nucleotide metabolism. GIP (genetic information processing, green): CHP chaperones, RMT RNA maturation, RRR replication, repair, recombination, TC transcription, TL translation. TP\_CP (transport and cellular processes, red): CP cellular processes, SEC protein secretion, MOT motility, TP small molecule transport. ENV (environmental information processing, gray): REG gene regulation, SIG signal transduction. MIS (miscellaneous functions, purple): GEN general enzymatic function: ISH transposases and ISH-encoded proteins, MIS miscellaneous. UNASS (unassigned function, yellow): CHY conserved hypothetical protein, HY hypothetical protein.

showed no evident phenotype under laboratory conditions, except for a mild increase in resistance to cefotaxime. However, GlpG was shown to cleave heterologous substrates. Specific targets of other Rho, such as Spitz, Gurken and Keren of *D. melanogaster*, were proteolytically processed by GlpG.<sup>11</sup> A chimeric protein, consisting of the N-terminal and periplasmically localized  $\beta$ -lactamase domain, a LacY-derived transmembrane segment (TMS), and a cytoplasmic maltose binding protein domain, could be cleaved *in vitro* by this Rho,<sup>12</sup> and in addition, GlpG could cleave truncated forms of the transporter protein MdfA.<sup>13</sup> In *Bacillus subtilis*, a rhomboid protease gene (*yggP*) null mutant displayed a cell division defect and decreased glucose uptake.<sup>14</sup> *Mycobacterium smegmatis* rhomboid null mutants exhibited impaired biofilm formation and augmented antibiotic sensitivity.<sup>15</sup>

The Rho family is widely represented through archaeal genomes.<sup>16</sup> Particularly, the halophilic model archaeon *Haloferax volcanii* encodes two Rho homologues, HVO\_1474 (RhoI) and HVO\_0727 (RhoII). We have previously obtained and characterized a Rho mutant deleted in the *rhoII* gene in *H. volcanii*. The mutant strain (MIG1) showed reduced motility on soft agar plates and increased novobiocin sensitivity and a truncation in a novel oligosaccharide bound to position N732 of the S-layer glycoprotein (SLG).<sup>17</sup> However, global changes on the proteome that may explain these phenotypes still need to be determined.

Comparative proteomics is a valuable tool to analyze the impact of the absence/overexpression of a particular protease on the proteome of a certain organism and allows for identification of putative endogenous substrates. In the case of processive proteases, accumulation of a particular protein in a protease defective strain with respect to the control strain would be an evidence of that protein being a specific substrate. This method was applied by our group to identify candidate targets of the LonB protease in *H. volcanii*.<sup>18</sup> On the other hand, the situation for regulatory enzymes, such as Rho, is

different. These proteases cut at specific sites releasing or exposing fragments of the substrate, and therefore, protease activity may be evidenced by changes in electrophoretic migration or stability of the (unprocessed) substrate protein.

In this work, a quantitative high-throughput comparative proteomics approach was applied in *H. volcanii* to understand the importance of Rho in archaeal physiology and to identify putative natural targets of RhoII.

## 2. EXPERIMENTAL SECTION

### 2.1. Strains and Growth Conditions

*H. volcanii* H26 (DS70  $\Delta$ pyrE2)<sup>19</sup> and MIG1<sup>17</sup> were grown in MGM 18% or Hv-Min medium<sup>20</sup> at 42 °C and 150 rpm. When needed, uracil or tryptophan (50  $\mu$ g/mL) was added to Hv-Min.

*E. coli* DH10 $\beta$  (Invitrogen) and GM33 (Marinus, 1973) were grown in Luria–Bertani (LB) medium at 37 °C and 150 rpm. Kanamycin (50  $\mu$ g/mL) or ampicillin (100  $\mu$ g/mL) was added to the medium when indicated. *E. coli* cells were transformed by the CaCl<sub>2</sub> method.<sup>21</sup>

### 2.2. Cell Fractionation

*H. volcanii* cultures were grown up to the indicated optical density at 600 nm (OD<sub>600</sub>), and cells were harvested by centrifugation (10 000  $\times$  g 10 min, 4 °C). Culture medium was recentrifuged under the same conditions, and the supernatant was passed through a 0.22  $\mu$ m nitrocellulose filter and precipitated with TCA 10% (v/v). Precipitated proteins were washed twice with 80% (v/v) acetone and left to dry 30 min at room temperature. Cell pellets were resuspended in 50 mM HCl-Tris, 2 M NaCl (pH 7.5), and disrupted by ultrasound (3  $\times$  30 s, 80 W). Lysates were clarified (17 000  $\times$  g for 20 min at 4 °C), and membranes were pelleted by centrifugation (100 000  $\times$  g for 1 h at 4 °C). The membranes were washed with the same buffer and both, supernatant (cytoplasmic fraction) and membranes, were recentrifuged for 30 min in the

same conditions. To remove remaining salts, cytoplasm and membrane proteins were precipitated overnight with 100% acetone at 4 °C followed by centrifugation ( $17\,000 \times g$  for 20 min at 4 °C). The precipitated proteins were washed twice with 80% (v/v) and once with 100% acetone and left to dry for 30 min at room temperature. All samples were resuspended in 1× SDS-PAGE loading buffer<sup>22</sup> containing 0.1% (w/v) SDS and 0.1 M DTT, incubated for 10 min at 70 °C, and conserved at −20 °C until use.

### 2.3. SDS-PAGE

Samples (30 µg per lane) were loaded onto 10% (w/v) polyacrylamide gels containing 0.1% SDS. The gels were run at room temperature (20 mA) until samples passed the stacking gel and all proteins were concentrated into one protein band in the separation gel. For the PROTOPAP assay,<sup>23</sup> samples were allowed to run 2 cm beyond the stacking gel (Figure S1). Proteins were visualized with a Coomassie brilliant blue (CBB-G250) stain.<sup>24</sup>

### 2.4. In-Gel Tryptic Digestion

Protein bands were excised from the gels and cut into small cubes (ca.  $1 \times 1 \text{ mm}^2$ ), which were completely destained according to Schluesener and colleagues.<sup>25</sup> In the case of PROTOPAP assay, each lane was divided in four 0.5 cm sections, which were treated separately in the same manner (Figure 1). Gel pieces were dried by incubation with 100% acetonitrile for 10 min at room temperature and then incubated with 50 mM DTT in 25 mM  $\text{NH}_4\text{HCO}_3$  (30 min at 60 °C) to reduce proteins disulfide bonds. The gel pieces were dried again with acetonitrile, and proteins were alkylated treating the gel pieces with 50 mM iodoacetamide in 25 mM  $\text{NH}_4\text{HCO}_3$  (1 h at room temperature in darkness). After washing (with destaining solution) and drying the gel pieces in a SpeedVac, trypsin (porcine, sequencing grade, Promega) solution (12.5 ng  $\text{mL}^{-1}$  in 25 mM ammonium bicarbonate, pH 8.6) was added. Protein digestion and peptide elution were performed according to Cerletti et al.<sup>18</sup> The extracted peptides were dried using a SpeedVac and stored at −20 °C. Before MS-analysis, peptides were resuspended in 20 µL of buffer A (0.1% formic acid in water, ULC/MS, Biosolve, Netherlands) with 2% (v/v) acetonitrile by sonication for 10 min and transferred to LC-MS grade glass vials (12 × 32 mm<sup>2</sup> glass screw neck vial, Waters, USA). Each measurement was performed with 8 µL of sample.

### 2.5. One-Dimensional nLC-ESI-MS/MS

An UPLC HSS T3 column (1.8 µm, 75 µm × 150 mm, Waters, Milford, MA, USA) and an UPLC Symmetry C<sub>18</sub> trapping column (5 µm, 180 µm × 20 mm, Waters, Milford, MA, USA) for LC as well as a PicoTip Emitter (SilicaTip, 10 µm i.d., New Objective, Woburn, MA, USA) were used in combination with the nanoACQUITY gradient UPLC pump system (Waters, Milford, MA, USA) coupled to a LTQ Orbitrap Elite mass spectrometer (Thermo Fisher Scientific Inc., Waltham, MA, USA). For elution of the peptides, a linear gradient with increasing concentration of buffer B (0.1% formic acid in acetonitrile, ULC/MS, Biosolve, Netherlands) from 1% to 40% within 165 min was applied, followed by a linear gradient from 40% to 99% acetonitrile concentration within 15 min (0–5 min, 1% buffer B; 5–10 min, 5% buffer B; 10–165 min, 40% buffer B; 165–180 min, 99% buffer B; 180–195 min, 1% buffer B) at a flow rate of 400 nL  $\text{min}^{-1}$  and a spray voltage of 1.5–1.8 kV. The column was re-equilibrated at 1% buffer B within 15

min. The analytical column oven was set to 55 °C, and the heated desolvation capillary was set to 275 °C. The LTQ Orbitrap Elite via instrument method files of Xcalibur (Rev. 2.1.0) in positive ion mode. The linear ion trap and Orbitrap were operated in parallel, that is, during a full MS scan on the Orbitrap in the range of 150–2000  $m/z$  at a resolution of 240 000 MS/MS spectra of the 20 most intense precursors, from most intense to least intense, were detected in the ion trap. The relative collision energy for collision-induced dissociation (CID) was set to 35%. Dynamic exclusion was enabled with a repeat count of 1 and 60 s exclusion duration window. Singly charged and ions of unknown charge state were rejected from MS/MS.

### 2.6. Protein Identification and Quantification

Protein identification was performed by SEQUEST<sup>26</sup> and MS Amanda<sup>27</sup> algorithms embedded in Proteome Discoverer 1.4 (Thermo Electron) searching against the complete proteome database of *H. volcanii* DS2 containing 4035 entries exported from the Halolex database<sup>28</sup> on September 24, 2013. The mass tolerance for precursor ions and fragment ions was set to 6 ppm and 0.4 Da, respectively. Only tryptic peptides with up to two missed cleavages were accepted. As static peptide modification the carbamidomethylation of cysteine and as variable peptide modification the oxidation of methionine as well as the conversion of glutamine (Gln) to pyro-glutamate (pyro-glu) at any N-terminus were admitted. The false discovery rate (FDR) was determined with the percolator validation in Proteome Discoverer 1.4 and the  $q$ -value was set to 1%.<sup>29</sup> For protein identification, the mass spec format-(msf)-files were filtered with peptide confidence “high” and two different peptides per protein. Additionally, protein grouping options were enabled as default, which means consider only PSMs (peptide scoring mass spectrum matches) with confidence at least “medium” and consider only PSMs with delta CN better than 0.15. Proteins were quantified by spectral counting,<sup>30,31</sup> and a protein was considered as significantly regulated at a  $p$ -value  $\leq 0.05$  (Student's  $t$  test) and fold  $\geq 1.5$ . Only proteins that had on average at least five PSMs were taken into consideration.

### 2.7. Generation of an Expression Vector of His Tagged PrsW

The predicted PrsW protease gene (HVO\_0408) was PCR-amplified from *H. volcanii* H26 genomic DNA. The amplicon (1038 bp) was synthesized using primers FWPrsWNcoI (5' ATATCCATGGACCAGCAGGACCCA 3') and RvPrsWBamHI (5' ATATGGATCCTCAGTCCTCGAACTCG 3') in a reaction mixture containing Phusion GC buffer (1×), 0.2 mM dNTPs, 0.6 mM of each primer 4% (v/v) DMSO and 0.5 units of Phusion DNA polymerase (New England Biolabs) in a final volume of 25 µL. The program used was 98 °C (30 s), 30 cycles of 98 °C (10 s)-60 °C (30 s)-72 °C (30 s) and a final extension of 72 °C (1 min). The PCR product was cloned in the ZeroBlunt TOPO cloning vector (ThermoFisher, Inc.). The identity of the amplification product was confirmed by sequencing (Macrogen, Korea). The DNA fragment corresponding to PrsW was excised from the ZeroBlunt TOPO by digestion with NcoI and BamHI and subcloned with an N-terminal 6× his tag in the *H. volcanii* expression vector pTA963.<sup>32</sup> The ligation product was transformed into *E. coli* DH10β and then passed through *E. coli* GM33 to obtain nonmethylated DNA and finally introduced in *H. volcanii* H26 or MIG1 by the standard PEG method.<sup>20</sup>



Table 1. Differential Subproteome of *H. volcanii* MIG1 Strain<sup>a</sup>

ID	gene name	description	TMS	signal peptide	lipobox	FC	SC	p-value	fold
Supernatant Exponential									
HVO_0874		Beta-lactamase domain protein/mRNA 3-end processing factor homologue				MIS	GEN	0.000136	17.8
HVO_2375	<i>pstS1</i>	ABC-type transport system periplasmic substrate-binding protein (probable substrate phosphate)		Tat	yes	TP_CP	TP	0.000013	11.4
HVO_2563	<i>rpl4</i>	50S ribosomal protein L4				GIP	TL	0.047086	1.7
Membrane Exponential									
HVO_1038	<i>udg4</i>	Uracil-DNA glycosylase superfamily protein				MIS	GEN	0.000666	28.7
HVO_1344		SBDS family protein				MIS	GEN	0.001658	18.1
HVO_2150	<i>hcpG</i>	Halocyanin	1	Tat		MET	EM	0.000016	7.8
HVO_2464	<i>sucD</i>	Succinate-CoA ligase (ADP-forming) alpha subunit				MET	CIM	0.041494	7.1
HVO_1925		Probable GTP-binding protein				MIS	GEN	0.042352	2.6
HVO_2757	<i>rpl1</i>	50S ribosomal protein L1				GIP	TL	0.008677	1.9
HVO_0316	<i>atpA</i>	A-type ATP synthase subunit A				MET	EM	0.049824	1.6
HVO_0570		Histidine kinase	3	Sec		ENV	SIG	0.043555	-1.5
HVO_0684	<i>gatB, aatB</i>	Aspartyl/glutamyl-tRNA(Asn/Gln) amidotransferase subunit B				GIP	TL	0.020533	-1.5
HVO_A0045	<i>htpX3</i>	HtpX-like protease	4			MIS	MIS	0.024904	-1.6
HVO_A0208	<i>cas5</i>	CRISPR-associated endoribonuclease Cas5, Hmari subtype				MIS	MIS	0.005354	-1.6
HVO_0194	<i>orc9</i>	Orc1-type DNA replication protein				MIS	MIS	0.026537	-1.8
HVO_0237		UPF0761 family protein				MIS	GEN	0.029733	-1.8
HVO_1357		receiver/bat box HTH-10 family transcription regulator				ENV	REG	0.04533	-1.8
HVO_B0052		PQQ repeat protein				MIS	GEN	0.043425	-1.9
HVO_0581	<i>ftsZ2</i>	cell division protein FtsZ, type II				MIS	MIS	0.024353	-2
HVO_1554	<i>traB</i>	TraB family protein	8			MIS	GEN	0.026824	-2
HVO_0874		beta-lactamase domain protein/mRNA 3-end processing factor homologue				MIS	GEN	0.045002	-2.6
HVO_0598		conserved hypothetical protein				UNASS	CHY	0.000252	-7.1
HVO_0762		NUDIX family hydrolase				MIS	GEN	0.000355	-8.4
HVO_1659	<i>mcsS2</i>	mechanosensitive channel protein MscS	5	Sec		TP_CP	TP	0.000240	-9
HVO_1997		Abi/CAAX family protein	7			MIS	GEN	0.026824	-10.7
HVO_0255		Spermine/spermidine synthase family protein	7			MIS	GEN	0.000011	-10.8
HVO_0477	<i>pepB3</i>	Aminopeptidase (homologue to leucyl aminopeptidase/aminopeptidase T)				MIS	GEN	0.000214	-13.1
HVO_B0273		Sensor box histidine kinase	7			ENV	SIG	0.047159	-13.9
HVO_1382	<i>nac</i>	Nascent polypeptide-associated complex protein				GIP	TL	0.003979	-14.9
HVO_2060	<i>agl8</i>	NUDIX family hydrolase (low-salt glycan biosynthesis protein Agl8)				MIS	MIS	0.034081	-19.3
HVO_0941		Conserved hypothetical protein	6			UNASS	CHY	0.000550	-24.1
HVO_2318	<i>uppS2</i>	Tritrans,polycis-undecaprenyl-diphosphate synthase				MET	LIP	0.043265	-25.4
HVO_1676	<i>tfb2</i>	Transcription initiation factor TFB				GIP	TC	0.006282	-27.1
HVO_0408		PrsW family protein	9			MIS	GEN	0.000165	-28.2
Cytoplasm Exponential									
HVO_2548	<i>rpl6</i>	50S ribosomal protein L6				GIP	TL	0.000076	9.5
HVO_2772		rhodanese domain protein/probable metallo-beta-lactamase family hydrolase				MIS	GEN	0.000001	9.2
HVO_C0074	<i>dppDF16</i>	ABC-type transport system ATP-binding protein (probable substrate dipeptide/oligopeptide)				TP_CP	TP	0.000001	9.2
HVO_2600	<i>map</i>	methionyl aminopeptidase				MIS	MIS	0.000035	8.5
HVO_1758	<i>trxB5</i>	oxidoreductase (homologue to thioredoxin-disulfide reductase)				MIS	GEN	0.000004	7.8
HVO_2709		GNAT family acetyltransferase				MIS	GEN	0.000104	6.9
HVO_0818	<i>thrC2</i>	threonine synthase				MET	AA	0.049049	4.9
HVO_1047	<i>qor2</i>	NADPH:quinone reductase				MIS	MIS	0.047097	4.8
HVO_1604	<i>aspC1</i>	pyridoxal phosphate-dependent aminotransferase (probable aspartate aminotransferase)				MIS	GEN	0.044358	2
HVO_A0406		conserved hypothetical protein				UNASS	CHY	0.010564	2
HVO_2270	<i>rmeM</i>	type I restriction-modification system DNA-methyltransferase RmeM				MIS	MIS	0.008658	1.9
HVO_0353	<i>rps12</i>	30S ribosomal protein S12				GIP	TL	0.024019	1.8
HVO_1478	<i>tfb5</i>	transcription initiation factor TFB				GIP	TC	0.049709	1.7
HVO_1681		DNA N-glycosylase				GIP	RRR	0.038567	1.6

Table 1. continued

ID	gene name	description	TMS	signal peptide	lipobox	FC	SC	p-value	fold
Cytoplasm Exponential									
HVO_2345		flavin-dependent pyridine nucleotide oxidoreductase				MIS	GEN	0.041979	1.6
HVO_0710	<i>pabB</i>	aminodeoxychorismate synthase component II				MET	COM	0.049446	1.5
HVO_1249		conserved hypothetical protein				MIS	GEN	0.025429	1.5
HVO_1488	<i>gnaD</i>	D-glucuronate dehydratase				MET	CHM	0.002489	−1.5
HVO_A0379	<i>hyuA2</i>	N-methylhydantoinase A (ATP-hydrolyzing)				MIS	MIS	0.013225	−1.5
HVO_2790	<i>apbC1</i>	Fe–S cluster carrier protein ApbC				MIS	MIS	0.012758	−1.6
HVO_2059	<i>agl12, rfbB</i>	dTDP-glucose 4,6-dehydratase (Agl12)				MET	CHM	0.036699	−1.7
HVO_2947	<i>pheT</i>	phenylalanine–tRNA ligase beta subunit				GIP	TL	0.0382	−1.8
HVO_0214		L-lactate dehydrogenase		Sec		MET	CIM	0.004094	−1.9
HVO_2695	<i>tsgA3</i>	ABC-type transport system periplasmic substrate-binding protein (probable substrate sugar)		Tat	yes	TP_CP	TP	0.027275	−2
HVO_1401	<i>tsgA11</i>	ABC-type transport system periplasmic substrate-binding protein (probable substrate sugar)		Tat	yes	TP_CP	TP	0.003844	−2.1
HVO_2740	<i>ndk</i>	nucleoside-diphosphate kinase				MET	NUM	0.019173	−2.2
HVO_1311		probable oxidoreductase (short-chain dehydrogenase family)				MIS	GEN	0.032821	−6
HVO_2684		UspA domain protein				MIS	GEN	0.000151	−9.1
HVO_2648	<i>serA2</i>	phosphoglycerate dehydrogenase				MIS	GEN	0.000035	−9.4
Supernatant Stationary									
HVO_0062	<i>dppA1</i>	ABC-type transport system periplasmic substrate-binding protein (probable substrate dipeptide/oligopeptide)		Tat	yes	TP_CP	TP	0.031260	1.7
HVO_1976	<i>secD</i>	Protein-export membrane protein SecD	5	Sec		TP_CP	SEC	0.047004	−5.3
HVO_1210	<i>flgA1</i>	Flagellin 1	1			TP_CP	MOT	0.000004	−5.3
HVO_1477		Endonuclease domain protein		Sec	yes	MIS	GEN	0.000004	−5.3
HVO_2607		PQQ repeat protein		Tat	yes	MIS	GEN	0.000004	−5.3
HVO_0058	<i>dppF1</i>	ABC-type transport system ATP-binding protein (probable substrate dipeptide/oligopeptide)				TP_CP	TP	0.000086	−6.0
HVO_A0181		Conserved hypothetical protein		Tat	yes	UNASS	CHY	0.000369	−6.0
HVO_A0377	<i>hyuE</i>	Hydantoin racemase				MIS	MIS	0.000608	−6.5
HVO_2384		CBS domain protein				MIS	GEN	0.000010	−6.7
HVO_2603	<i>sec11a</i>	Signal peptidase I	1			TP_CP	SEC	0.000010	−6.7
HVO_1945		Conserved hypothetical protein		Tat	yes	UNASS	CHY	0.000144	−6.7
HVO_2413	<i>tef1a2</i>	Translation elongation factor aEF-1 alpha subunit				GIP	TL	0.035008	−7.0
HVO_2286		Conserved hypothetical protein		Tat	yes	UNASS	CHY	0.027060	−7.4
HVO_1153		Conserved hypothetical protein	1			UNASS	CHY	0.000002	−7.5
HVO_0054	<i>glyS</i>	Glycine–tRNA ligase				GIP	TL	0.000377	−7.8
HVO_B0057	<i>cbiH2, cobJ2</i>	Precorrin-3B C17-methyltransferase				MET	COM	0.000124	−8.7
HVO_2815	<i>hbd1</i>	3-hydroxyacyl-CoA dehydrogenase/enoyl-CoA hydratase				MET	LIP	0.000706	−8.9
HVO_0348	<i>rpoB1</i>	DNA-directed RNA polymerase subunit B'				GIP	TC	0.000865	−9.0
HVO_2471	<i>pccB2</i>	Propionyl-CoA carboxylase carboxyltransferase component				MET	LIP	0.033685	−9.1
HVO_2554	<i>rpl14</i>	50S ribosomal protein L14				GIP	TL	0.000011	−9.5
HVO_B0184	<i>dppA14</i>	ABC-type transport system periplasmic substrate-binding protein (probable substrate dipeptide/oligopeptide)		Tat	yes	TP_CP	TP	0.000573	−10.1
HVO_B0061	<i>cbiL</i>	Precorrin-2 C20-methyltransferase				MET	COM	0.000175	−10.2
HVO_2749	<i>rpl21e</i>	50S ribosomal protein L21e				GIP	TL	0.000001	−10.3
HVO_2452	<i>nrdJ</i>	Ribonucleoside-diphosphate reductase, adenosylcobalamin-dependent				MET	NUM	0.036975	−11.9
Membrane Stationary									
HVO_0887	<i>korB</i>	oxoglutarate–ferredoxin oxidoreductase beta subunit				MET	CIM	0.006496	1.7
HVO_2614	<i>udp2</i>	uridine phosphorylase				MET	NUM	0.023086	1.5
HVO_2989	<i>pmm4</i>	phosphohexomutase (phosphoglucosylmutase/phosphomannomutase)				MET	CHM	0.040726	−1.5
HVO_2069		RND superfamily permease	11			TP_CP	TP	0.002656	−1.6
HVO_C0054		hypothetical protein		Tat		UNASS	HY	0.033063	−1.6
HVO_0307		conserved hypothetical protein		Sec		UNASS	CHY	0.022016	−2
HVO_1751	<i>copA</i>	P-type transport ATPase (probable substrate copper/metal cation)	8			TP_CP	TP	0.011109	−2.1
HVO_0462	<i>cydA</i>	cytochrome bd ubiquinol oxidase subunit I	9			MET	EM	0.000721	−8.8
HVO_B0228	<i>tsgA9</i>	ABC-type transport system periplasmic substrate-binding protein (probable substrate sugar)		Tat	yes	TP_CP	TP	0.000374	−8.8

Table 1. continued

ID	gene name	description	TMS	signal peptide	lipobox	FC	SC	p-value	fold
Membrane Stationary									
HVO_1870		probable metalloprotease	7			MIS	GEN	0.000041	−9.9
Cytoplasm Stationary									
HVO_1804	<i>pncB</i>	nicotinate phosphoribosyltransferase				MET	COM	0.000018	8.2
HVO_2639		DUF1611 family protein				MIS	GEN	0.0001	6.7
HVO_2860		DUF181 family protein				MIS	GEN	0.0001	6.7
HVO_0087	<i>hemB</i>	porphobilinogen synthase				MET	COM	0.0376	−1.5
HVO_1575	<i>rocF</i>	Arginase				MET	AA	0.0356	−1.5
HVO_2225		AstE family protein				MIS	GEN	0.0232	−1.8

“Regulation factors for three biological replicates from H26 and MIG1 strains were submitted to a Student’s *t*-test. Proteins with *p*-values  $\leq 0.05$  were considered significant. Negative fold values indicate that the protein is less abundant in the mutant than in the wt, whereas a positive fold value indicates accumulation of the protein in MIG1. For membrane fractions, two independent experiments (three biological replicates each) were performed, and data corresponding to both assays were included in the table. TMS: number of transmembrane segments. Sec: general translocation signal peptide. Tat: Twin arginine translocation signal peptide. FC and SC: functional class and functional sub-class, according to the Halolex database, respectively (for abbreviations, see Figure 1).

## 2.8. Protein Stability Determination

*H. volcanii* H26 and MIG1 harboring the pTA963-PrsW his tagged construction were grown until they reached a OD<sub>600</sub> of 0.3–0.5, and then 1 mM tryptophan was added and left O/N to induce the *p<sub>tnaA</sub>* promoter. After incubation with tryptophan, 100 µg/mL puromycin was added to the cultures. Samples (5 mL) were taken at the indicated times, and membrane fractions were obtained as detailed above.

## 2.9. Western Blotting

Polyacrylamide gels (12% w/v) were transferred to PVDF membranes (80 mA, 2h) and blocked with TBST buffer [25 mM Tris-HCl, pH 7.4, 0.01% (v/v) Tween 20]] with 5% (w/v) skimmed milk. Membranes were incubated with 1:5000 anti-His antibody (Biolegend) in blocking buffer, washed with TBST (3 × 10 min), and incubated with 1:10 000 alkaline phosphatase-conjugated antimouse IgG (Sigma-Aldrich) for 2 h. After washing (TBST, 3 × 10 min), blots were developed with 0.33 mg/mL nitro blue tetrazolium and 0.01 mg/mL 5-bromo-4-chloro-3-indolyl-phosphate.

## 2.10. Cell Adhesion Assay

Surface adhesion was assessed based on the method described by Tripepi et al.<sup>33</sup> *H. volcanii* cultures (3 mL) at an OD<sub>600</sub> of ~0.3 were incubated in 50 mL sterile screw cap plastic tubes. Glass coverslips were inserted into each tube at an angle of 90° and were incubated without shaking. After the indicated time intervals, coverslips were removed with forceps, submerged for 2 min in 2% (v/v) acetic acid, and allowed to air-dry. Dry coverslips were stained in 0.1% (w/v) crystal violet for 10 min, washed (×3) with distilled water, air-dried, and then observed by light microscopy using a Nikon Eclipse Ti microscope.

## 3. RESULTS AND DISCUSSION

### 3.1. Global Analysis of Total Proteins Identified in *H. volcanii* wt and $\Delta$ rhoII (MIG1) Strains

To investigate the relevance of Rho in *H. volcanii* physiology, the differential proteome map between the parent (H26) and a mutant strain (MIG1) containing a chromosomal deletion in one of the two Rho homologue genes, *rhoII* (HVO\_0727), was assessed. Culture media supernatant, membrane, and cytoplasmic proteins obtained from triplicate cultures of both strains harvested in exponential (exp) (OD<sub>600</sub> 0.5–0.6) and stationary (st) (OD<sub>600</sub> 1.8–1.9) growth phases were subjected to SDS-

PAGE, digested with trypsin, and then analyzed by nLC–MS/MS as described in the Experimental Section. As Rho exert their proteolytic activity within the membrane environment, their natural substrates are expected to be integral membrane proteins. Thus, to analyze the membrane fraction in more detail in search of putative RhoII direct targets, the same assay was repeated only with membrane fractions (triplicates) from *H. volcanii* H26 and MIG1 at exp growth phase.

Out of 4035 total proteins from the predicted *H. volcanii* proteome, 1847 (45.8%) were identified including all strains, growth phases, and cell fractions of both experiments. The complete list of detected proteins is included in Table S1. From these, 276 (14.9%) are predicted to be integral membrane proteins, 133 (7.2%) membrane-associated either by a predicted signal peptide or lipobox, and the remaining 1438 (77.8%) as soluble proteins (Table S1). Figure 1 shows the number of identified proteins distributed according to strain and growth phase (Figure 1A) and functional category (Figure 1B). The protease RhoII (HVO\_0727) was not detected in membrane fractions of *H. volcanii* H26 (exp and st phase) in either of the two assays. This outcome was not unexpected since integral membrane proteins containing several TMS or hydrophobic stretches, such as RhoII, are hardly detected by MS technology, as they are under-represented in trypsin digestion products.<sup>34</sup> However, when these samples were used in a PROTOMAP assay, RhoII was detected in the parental strain but not in the mutant confirming the absence of this protease in MIG1 (see further).

### 3.2. Proteins Differentially Represented in *H. volcanii* RhoII Deficient Strain

Using the criteria described in M and M, a total of 103 proteins were differentially represented between the *H. volcanii* H26 parent and MIG1 strains. Table 1 shows the proteins that evidenced significant variation in amount, organized by growth phase and cellular fraction. Thirty-three proteins (4 from culture medium supernatants, 9 from membrane, and 20 from cytoplasm) were enriched, while 70 proteins (23 from culture medium supernatant, 32 from membrane, and 15 from cytoplasm) decreased their concentration. Most of the proteins that showed variation in their concentration were detected in membrane fractions, in accordance with RhoII exerting its role within the membrane.

The proteins differing between strains in the exp and st growth phases were not coincident, suggesting a growth phase-

dependent effect of the *rhoII* knockout (Table 1). The impact of the RhoII protease deficiency in cytoplasm and membrane protein samples was more evident in vegetative cells (exp phase) than in nonactively growing cells (st phase) since 60 versus 16 proteins varied in abundance, respectively. The opposite situation was observed for the secretome fraction in which only three proteins were differential (accumulated) in vegetative cells, while 24 varied in concentration (1 increased and 23 decreased) in st phase cultures. It is likely that changes in the cell proteome, produced in absence of *rhoII* during the exp growth phase, may be reflected on the secretome of the mutant at a later stage of growth. A volcano plot (Figure 2) was

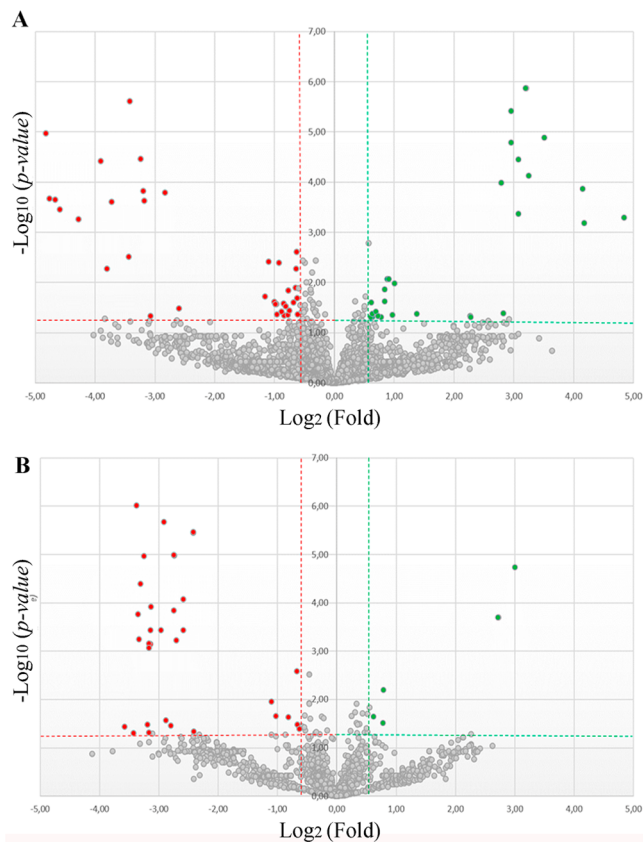


**Figure 2.** Graphical representation of quantitative proteomics data. Total detected proteins from (A) exp and (B) st growth phases are ranked in a volcano plot according to their statistical  $p$ -value ( $\log_{10}$ ) and their relative abundance ratio ( $\log_2$  fold change) between MIG1 and H26 strains ( $x$ -axis). Off-centered spots are those that vary the most between both groups. Each data point represents a single unique protein identified in our proteomic analysis, color coded as follows: gray indicates no significant change and colored dots indicate significant negative (red) and positive (green) changes.

generated to visualize the data set changes obtained in these experiments, by plotting  $-\log_{10}(p\text{-value})$  versus  $\log_2$  (fold-change) for proteins differentially detected in MIG1 samples taken in exp (Figure 2A) and st (Figure 2B) phases of growth. Of those proteins meeting statistically significant criteria ( $p\text{-value} \leq 0.05$ ; fold  $\geq 1.5$ ), 63 were detected in exp phase (27 over-represented, 36 under-represented) and 40 in st phase (6 enriched, 34 under-represented).

The differential proteins belonged to several functional classes (Figure 3, Table 1). Even though the majority of these proteins corresponded to the miscellaneous and general

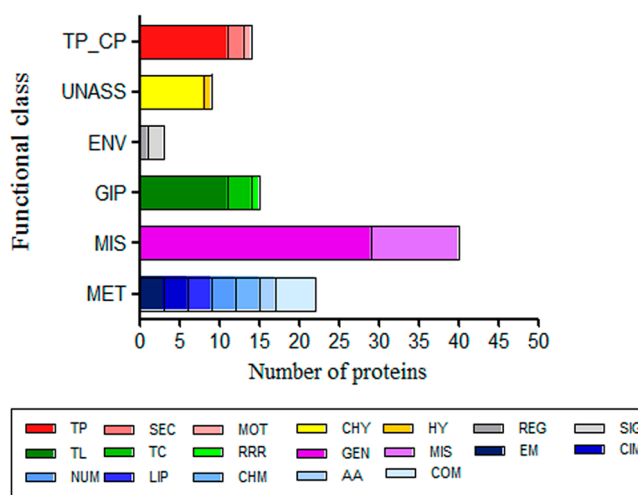


**Figure 3.** Distribution of the MIG1 differentially expressed proteins into functional classes, according to the Halolex database. For abbreviations, see Figure 1.

metabolic pathways, proteins involved in translation and solute transport were the most represented, suggesting that these processes are affected by RhoII. However, the growth performance of the mutant was not affected at standard laboratory conditions,<sup>17</sup> probably due to a functional overlap between the two Rho homologues present in *H. volcanii*.

In cytoplasm fractions, 35 proteins were differentially represented in the mutant cells. As all Rho substrates identified so far are integral membrane proteins, these differential proteins are probably a consequence of yet unidentified proteolytic or gene expression processes regulated by RhoII, representing an indirect/secondary effect of the knockout mutation.

Differential proteins with predicted TMS that may have been released to the cytoplasm as a consequence of RhoII activity were not identified in the cytoplasm. This observation suggests that, if present, they were either degraded or not detected under the experimental conditions used in this work.

The proteins that showed altered levels in the cytoplasm fractions were very diverse, and they could not be associated with a defined route or metabolic pathway.

### 3.3. Proteins Differentially Represented in the Membrane Fraction (Potential Direct Targets of RhoII)

A total of 41 proteins were affected by the *rhoII* mutation in membrane fractions (Table 1) comprising 40.2% of the total affected proteins in MIG1. Fourteen proteins detected as differential are predicted to have at least one TMS, and three (without TMS) contain signal peptides that likely target them to the cell surface. The remaining proteins affected in the mutant may be associated with the membrane via interactions with other molecules (i.e., lipids, other proteins) and likely represent indirect targets of RhoII. For instance, uracil DNA glycosylase (accumulated 28.7-fold in membranes of exponentially growing cells), which participates in DNA base excision repair, has been reported to be associated with the mitochondrial inner membrane through electrostatic interactions.<sup>36</sup> Nonetheless, it cannot be discarded that some of these proteins may represent contamination from cytoplasmic origin.

Rho are not processive proteases; therefore, their activity may expose or release a portion of the substrate, leading to



changes in size, stability, or location of the cleaved substrate protein. Consequently, integral membrane proteins, which evidenced variations in amount (accumulated or decreased), will be discussed as putative targets of RhoII. Proteins with altered electrophoretic migration were also taken into consideration (see next section).

Rho cleave target proteins within or near a TMS. Most characterized Rho substrates are single TMS, type I or III proteins (N-terminus facing the extracellular side with or without a signal peptide, respectively), even though exceptions are known such as *Drosophila melanogaster* Star, which is a type II membrane protein (N-terminus facing the intracellular side of the cell).<sup>57</sup> It has been proposed that Rho so far characterized from eukaryotes and bacteria recognize two elements in their natural substrates: part of the TMS and a sequence motif.<sup>38</sup>

Among the integral membrane proteins which evidenced differential levels between MIG1 and the parental strain, only HVO\_2150, encoding a halocyanin homologue, which accumulated in MIG1 (7.8-fold), fulfills the requirements to be a Rho substrate following the criteria proposed by Strisovsky et al.<sup>39</sup> (1TMS, type I or III membrane protein and presence of a 7 amino acid conserved motif).

Halocyanins are blue copper membrane associated proteins from halophilic archaea that are thought to act as mobile electron carriers in a way similar to plant plastocyanins.<sup>40</sup> Cu<sup>2+</sup> regulates plastocyanin abundance in cyanobacteria, algae, and higher plants, which show a decrease in plastocyanin abundance when subjected to Cu deficiency. However, the mechanism of down-regulation varies, as some organisms show Cu-induced variations in mRNA levels, while others evidence Cu deficiency-induced plastocyanin proteolysis.<sup>41–43</sup> In *Chlamydomonas*, Cu deficiency-induced proteolysis was proposed to be carried out by the IMP RSEP1 based in gene expression studies.<sup>42</sup> Halocyanin was purified from the haloalkaliphilic archaeon *Natronobacterium pharaonis* and the gene was cloned and sequenced;<sup>44</sup> however, regulation of halocyanin levels by Cu has not been confirmed in haloarchaea.

In *Arabidopsis* sp., mutations in two P-type ATPases (PAA1 and PAA2) that deliver Cu to the chloroplast and thylakoid lumen caused 80–90% reduction of plastocyanin abundance.<sup>45,46</sup> While plant chloroplast P-type ATPases import Cu to the chloroplast lumen, prokaryotic P-type ATPases contribute to Cu detoxification by copper efflux out of the cell.<sup>47</sup> In the thermophilic and thermoacidophilic archaea *Archaeoglobus fulgidus* and *Sulfolobus solfataricus*, CopA ATPases are active Cu export pumps that confer Cu and Ag tolerance.<sup>48,49</sup> In this study, a P-type ATPase (*copA*, HVO\_1751) showed a 2.1-fold reduction in abundance in the MIG1 strain (Table 1). A functional link between halocyanin and the CopA homologue in *H. volcanii* could be hypothesized. Whether RhoII regulates directly halocyanin concentration through processing or indirectly (i.e., by processing of a P-type ATPase and therefore regulating Cu and halocyanin levels) remains to be determined and is focus of future research.

*Escherichia coli* rhomboid GlpG was shown to cleave heterologous multi pass membrane proteins<sup>13</sup> and the rhomboid protease 1 (RHBDD1) was reported to cleave the six TMS TSAP6 protein in human cell lines, allowing for a probably TSAP6-dependent regulation of exosome trafficking.<sup>50</sup> Therefore, in addition to halocyanin, the polytopic integral membrane proteins, which evidenced variations in their

abundance in MIG1, were also considered as putative RhoII substrates.

Changes in the concentration of proteins involved in regulation of gene expression may explain differences in amount of the protein products of the genes they control. Two polytopic membrane sensor histidine kinases (HVO\_0570 and HVO\_B0273) were less abundant in MIG1 exp phase samples (Table 1) with negative folds of 1.5 and 13.9, respectively, and may represent RhoII direct targets. It has been reported that the Rho PARL mediates cleavage of the histidine kinase PINK1 in the mitochondrial inner membrane, which regulates the activity of respiratory complex I and the clearance of damaged mitochondria by mitophagy.<sup>51</sup>

Four integral membrane metalloproteases showed lower protein levels in MIG1 than in the parental strain (Table 1): peptidase T homologue (HVO\_0477, 13.1-fold), Abi/CAAX protease (HVO\_1997, 10.7-fold), HtpX- like protease (HVO\_A0045, 1.6-fold), and PrsW protease homologue (HVO\_0408, 28.2-fold), suggesting that metal-dependent proteolysis at the membrane level is, by some means, regulated by RhoII. This pattern may reflect a specific effect of RhoII on individual proteases but may also be a consequence of altered metal availability caused by variations in metal transporters (Table 1). It is likely that some proteins observed as stabilized in the mutant (Table 1) may accumulate as a consequence of the level reduction of these proteases. To the best of our knowledge, these enzymes have not been characterized in Archaea, and the fact that in this study they were detected at the protein level suggests that they are functional enzymes in *H. volcanii*.

In *Bacillus subtilis*, the PrsW peptidase inactivates the antisigma factor RsiW by performing the first of several proteolytic cleavages, which results in the transcription of genes controlled by the extra cytoplasmic function sigma factor  $\sigma^W$ .<sup>52</sup> To validate the results obtained in the proteomic approach, the *in vivo* stability of the *H. volcanii* PrsW protease was compared in the parental and MIG1 strains. Expression of the *prsW* gene, cloned with an N-terminal His tag downstream the *H. volcanii* tryptophanase promoter (*ptnA*), was induced in both strains by addition of tryptophan (1 mM) to the growth medium. Cells were treated with puromycin to block protein translation, and the stability of PrsW over time was assessed by Western blotting. While PrsW electrophoretic mobility was not affected in the mutant, the levels of PrsW were significantly reduced after 16 h (Figure 4) compared to the parental strain. This result correlates with the reduced PrsW levels observed in the mutant in the proteomic approach and suggests that PrsW is affected by RhoII, likely through a proteolytic signaling cascade at the membrane in *H. volcanii* cells. Alternatively, as the recombinant protein bears an N-terminal 6His tag, processing by RhoII of a small peptide from the C-terminus (not detected as a shift in migration in the SDS-PAGE) may increase the stability of PrsW in the parental strain. As the biological function of PrsW in archaea is not known, at present it is not possible to correlate/evaluate to what extent the deficiency in PrsW affects the physiology of the *H. volcanii* MIG1 mutant.

### 3.4. Proteins Differentially Represented in the Secretome of *H. volcanii*

The growth medium of *H. volcanii* MIG1 (exp plus st phases) showed 27 proteins with variations in their level, compared to the wt (Table 1). Out of these, eight are predicted secretory proteins, four are expected to be membrane associated via at



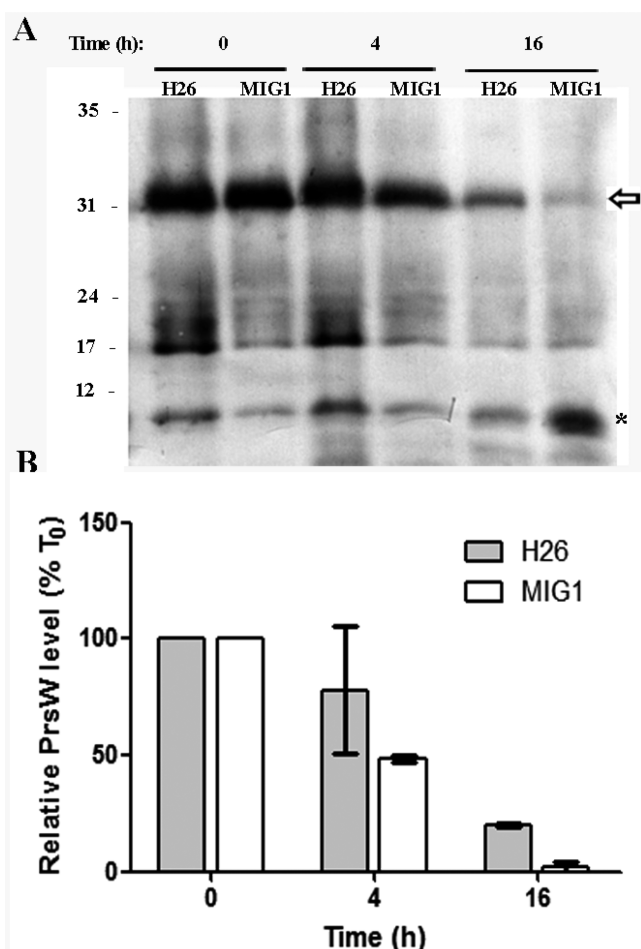


**Figure 4.** (A) Stability of PrsW homologue in MIG1 strain. *H. volcanii* H26 and MIG1 cells harboring plasmid pTA963 containing the *prsW* gene with a 6× histidine tag under the *ptnA* promoter were grown to exp phase in the presence of tryptophan 1 mM. At that point, puromycin (100  $\mu$ g/mL) was added, and samples were taken at the indicated times and subjected to SDS-PAGE followed by Western blotting with anti-his tag antibody. (B) Position of Molecular weight markers (kDa) is indicated at the left. The arrow points the band corresponding to PrsW and the asterisk a degradation product. The band corresponding to PrsW was quantified with ImageJ. The plotted data correspond to two independent experiments. Error bars, SD.

least one TMS, and the remaining are likely soluble proteins. The presence of proteins without a predicted signal peptide in culture medium supernatant is not uncommon; actually, evidence from proteomics studies suggests that there are significant differences between predicted and experimental archaeal secretomes.<sup>53,54</sup> These differences may be due to unconventional secretion such as vesicle transport or a consequence of cell lysis. In any case, soluble proteins (with or without a signal peptide) that displayed differences in their levels in MIG1 supernatants may represent an indirect effect of the *rhoII* deletion.

Four integral membrane proteins were underrepresented in MIG1 culture media supernatants (Table 1). Out of these, SecD (HVO\_1976), flagellin 1 (HVO\_1210), and signal peptidase I (HVO\_2603) were detected in both strains, while the conserved hypothetical protein (HVO\_1153) was not detected in the supernatants of MIG1 cultures. The absence of peptides from HVO\_1153 in the culture medium supernatant

of MIG1 could be a consequence of the lack of processing by RhoII.

SecD and Sec1a are proteins involved in the Sec protein translocation pathway.<sup>55,56</sup> Even though they were both affected in the mutant, the proteomic data did not provide additional evidence, suggesting that this pathway is altered in MIG1.

HVO\_1153 is a conserved hypothetical protein with 1 TMS. BLAST searches indicated that this protein has homology with archaeal flagellin domain-containing proteins and also with bacterial adhesins, and thus, the lack of processing of HVO\_1153 in MIG1 may contribute to the observed defects in motility and cell adhesion (see further) previously evidenced in the mutant. Amino acid sequence analysis with Pattenprot ([https://npsa-prabi.ibcp.fr/cgi-bin/npsa\\_automat.pl?page=/NPSA/npsa\\_pattenprot.html](https://npsa-prabi.ibcp.fr/cgi-bin/npsa_automat.pl?page=/NPSA/npsa_pattenprot.html)) evidenced the presence of a Rho consensus motif within the predicted TMS of this hypothetical protein. Thus, it can be hypothesized that the presence of peptides from HVO\_1153 in the culture medium of the wt strain may be due to RhoII proteolytic activity.

Flagellin 1 is the major component of the *H. volcanii* flagellum and deletion of the corresponding gene, *flgA1*, renders nonmotile cells.<sup>33</sup> Flagella are released from the cell surface through centrifugation; therefore, the reduced level of flagellin peptides in the culture supernatant of MIG1 suggests that flagella are either less abundant or not properly assembled, which may contribute with the reduced motility reported previously for this mutant.<sup>17</sup> Maturation of flagellin involves N-glycosylation and cleavage by PibD signal peptidase III prior to flagellum assembly.<sup>33</sup> Whether the role of RhoII regulating the level of flagellin in the culture medium is direct or indirect (i.e., regulating flagellin glycosylation and flagellum assembly) needs to be experimentally determined. This also applies to Sec11a and HVO\_1153, as both have predicted glycosylation sites, according to NetNGlyc server.<sup>57</sup>

### 3.5. Identification of Proteins with Differential Migration in the *H. volcanii rhoII* KO Mutant

Rho cleave their substrates at specific sites releasing peptides which often play a regulatory role.<sup>58</sup> Therefore, to detect variations in the electrophoretic migration of individual proteins that may arise from differential processing in the mutant versus wt strain, a simplified PROTOMAP assay was performed.<sup>23</sup> The results are shown in Table 2.

In this assay, RhoII (HVO\_0727) was detected in membranes from the parental strain, while it was not evidenced in MIG1, confirming the absence of the RhoII protease in this mutant. This finding agreed with the observation that a higher percentage of total proteins with predicted TMS were detected in this experiment compared to the previous analysis (21 vs 12%, respectively) (Tables S1 and S3).

A total of 99 proteins showed differences in amount (fold  $\geq 1.5$ ) in at least one of the gel sections (Table 2). Twenty-one integral membrane proteins displayed differences in comparing the mutant versus wt strain and may represent a direct consequence of RhoII proteolytic activity (absence/presence). In addition, 78 predicted soluble proteins showed differential migration in the PROTOMAP experiment. These probably represent proteins that were secondarily/indirectly affected by the *rhoII* deletion, as a consequence of absence of processing by other protease(s) or by another altered posttranslational modification process.

Table 2. Proteins with Differential Migration in SDS-PAGE in the MIG1 Mutant<sup>a</sup>

ID	gene name	protein name	TMS	signal peptide	lipobox	FC	SC	fold S1	fold S2	fold S3	fold S4	total fold
HVO_1240		Conserved hypothetical protein	0	Tat	yes	UNASS	CHY	8.8		1.8		ns
HVO_2545	<i>rpl18</i>	SOS ribosomal protein L18	0			GIP	TL	8.1				ns
HVO_2302		<b>Ubiquinone biosynthesis protein UbiB</b>	3			MET	COM	1.8				ns
HVO_1847	<i>pepF</i>	Oligoendopeptidase PepF	0			MIS	MIS	1.7				ns
HVO_2495		<b>DUF106 family protein</b>	4			MIS	GEN	-1.5				ns
HVO_0541	<i>citB2, acnA</i>	aconitate hydratase	0			MET	CIM	-1.5				ns
HVO_C0075	<i>dppA16</i>	ABC-type transport system periplasmic substrate-binding protein (probable substrate dipeptide/oligopeptide)	0	Tat	yes	TP_CP	TP	-1.5				ns
HVO_1469	<i>menD</i>	2-succinyl-5-enolpyruvyl-6-hydroxy-3-cyclohexene-1-carboxylate synthase	0			MET	COM	-1.6				-1.9
HVO_1242		Conserved hypothetical protein	0	Tat	yes	UNASS	CHY	-7.8				ns
HVO_0893	<i>mmcA1</i>	Methylmalonyl-CoA mutase subunit A	0			MET	CIM	-10.3				ns
HVO_C0074	<i>dppDF16</i>	ABC-type transport system ATP-binding protein (probable substrate dipeptide/oligopeptide)	0			TP_CP	TP	-14.4				ns
HVO_0519	<i>rpa2</i>	Replication protein A	0			GIP	RRR		7.1			ns
HVO_2784	<i>rps13</i>	30S ribosomal protein S13	0			GIP	TL		5.2			ns
HVO_0447	<i>phnD1</i>	ABC-type transport system periplasmic substrate-binding protein (probable substrate phosphate/phosphonate)	0	Tat	yes	TP_CP	TP		2.1			2.0
HVO_2945	<i>valS</i>	Valine-tRNA ligase	0			GIP	TL		1.8			ns
HVO_0220	<i>mcm</i>	ATP-dependent DNA helicase MCM	0			GIP	RRR		1.8			ns
HVO_1305	<i>porA</i>	Pyruvate-ferredoxin oxidoreductase alpha subunit	0			MET	CIM		1.8			ns
HVO_0133	<i>ftsI, ctfI</i>	Thermosome subunit 1	0			GIP	CHP		1.7			ns
HVO_1590	<i>dnaK</i>	DnaK-type molecular chaperone Hsp70	0			GIP	CHP		1.6			ns
HVO_2072	<i>csg</i>	<b>S-layer glycoprotein</b>	1	Sec		TP_CP	CE		1.5	1.7		ns
HVO_0717	<i>ftsZ1</i>	Cell division protein FtsZ, type 1	0			TP_CP	CP		1.5			ns
HVO_2209	<i>oadhA4</i>	Probable branched-chain amino acid dehydrogenase E1 component alpha subunit	0			MET	AA		-1.5			-1.6
HVO_A0379	<i>hyuA2</i>	N-methylhydantoinase A (ATP-hydrolyzing)	0			MIS	MIS		-1.5			ns
HVO_1304	<i>porB</i>	Pyruvate-ferredoxin oxidoreductase beta subunit	0			MET	CIM		-1.5			ns
HVO_0481	<i>gap2</i>	Glyceraldehyde-3-phosphate dehydrogenase (NAD) (phosphorylating)	0			MET	CIM		-1.5			ns
HVO_A0271	<i>glpC2</i>	Glycerol-3-phosphate dehydrogenase subunit C	0			MET	CIM		-1.5			-1.7
HVO_3007	<i>mdh</i>	Malate dehydrogenase	0			MET	CIM		-1.6			ns
HVO_1009		Probable oxidoreductase (aldo-keto reductase family protein)	0			MIS	GEN		-1.6	1.6		ns
HVO_2617		<b>TrkA-C domain protein</b>	3			MIS	GEN		-1.7			ns
HVO_2643	<i>qor1</i>	NADPH:quinone reductase	0			MIS	MIS		-1.7			ns
HVO_0243	<i>liaE</i>	Threonine aldolase	0			MET	AA		-1.8			-1.9
HVO_0832		Alpha/beta hydrolase fold protein	0	Sec		MIS	GEN		-1.8	-1.8		-1.6
HVO_0945	<i>chaA</i>	<b>ba3-type terminal oxidase subunit I</b>	14			MET	EM		-1.8			ns
HVO_0104	<i>radA</i>	DNA repair and recombination protein RadA	0			GIP	RRR		-1.9			ns
HVO_1573	<i>gyrA</i>	DNA gyrase subunit A	0			GIP	RRR		-2.2			ns
HVO_1631	<i>dph2</i>	S-adenosyl-L-methionine:L-histidine 3-amino-3-carboxypropyltransferase (GTP binding)	0			MIS	MIS		-5.2	5.8		ns
HVO_1675	<i>corA</i>	<b>Magnesium transport protein CorA</b>	2			TP_CP	TP		-5.2			-1.7
HVO_B0078	<i>dppF11</i>	ABC-type transport system ATP-binding protein (probable substrate dipeptide/oligopeptide)	0			TP_CP	TP		-5.4	13.6		ns
HVO_1443		ABC-type transport system ATP-binding protein	0			TP_CP	TP		-5.5			-2.0

Table 2. continued

ID	gene name	protein name	TMS	signal peptide	lipobox	FC	SC	fold S1	fold S2	fold S3	fold S4	total fold
HVO_2191	<i>purU</i>	Formyltetrahydrofolate deformylase	0			MET	NUM		-5.8			ns
HVO_1006		ABC-type transport system ATP-binding protein	0			TP_CP	TP		-6.3			ns
HVO_B0011	<i>soxA1</i>	Sarcosine oxidase	0			MET	AA		-6.3			-6.7
HVO_2168	<i>moxR3</i>	AAA-type ATPase (MoxR subfamily)	0			MIS	MIS		-6.4	13.8		ns
HVO_0951		<b>Hypothetical protein</b>	1			UNASS	HY		-6.5			-6.9
HVO_2993	<i>pihD</i>	<b>Prepilin peptidase PihD</b>	6			MIS	MIS		-7.7			-2.0
HVO_2348	<i>nptA</i> , <i>folE2</i>	GTP cyclohydrolase MptA	0			MET	COM		-12.4	9.0		-1.7
HVO_1576		NAD-dependent epimerase/dehydratase	0			MIS	GEN			17.4		2.3
HVO_2397	<i>znuA1</i>	ABC-type transport system periplasmic substrate-binding protein (probable substrate zinc)	0	Tat	yes	TP_CP	TP			14.6		ns
HVO_A0611	<i>znuA2</i>	ABC-type transport system periplasmic substrate-binding protein (probable substrate zinc)	0	Tat	yes	TP_CP	TP			9.6		ns
HVO_2374	<i>phoU2</i>	Transcription regulator (homologue to phosphate uptake regulator)	0			ENV	REG			9.0		ns
HVO_0739		<b>Conserved hypothetical protein</b>	4			UNASS	CHY			9.0		ns
HVO_2943	<i>pyrD</i>	Dihydroorotate dehydrogenase (quinone)	0			MET	NUM			7.9		ns
HVO_2607		PQQ repeat protein	0	Tat	yes	MIS	GEN			7.3		ns
HVO_2384		CBS domain protein	0			MIS	GEN			7.1		ns
HVO_2068	<i>fisZ8</i>	FtsZ family protein type III	0			MIS	GEN			6.1		ns
HVO_A0619		Conserved hypothetical protein	0	Tat	yes	UNASS	CHY			5.8		ns
HVO_2756	<i>np10</i>	50S ribosomal protein L10	0			GIP	TL			5.1		ns
HVO_1506	<i>ilvC</i>	Ketol-acid reductoisomerase	0			MET	AA			2.7		ns
HVO_1570	<i>top6A</i>	DNA topoisomerase VI subunit	0			GIP	RRR			2.4		ns
HVO_0059	<i>dppD1</i>	ABC-type transport system ATP-binding protein (probable substrate dipeptide/oligopeptide)	0			TP_CP	TP			1.9		ns
HVO_2046	<i>agI7</i>	Sulfatase domain protein	0			MIS	MIS			1.8		ns
HVO_2047		Conserved hypothetical protein	0			UNASS	CHY			-1.5		ns
HVO_2703	<i>panB2</i>	3-methyl-2-oxobutanoate hydroxymethyltransferase	0			MET	COM			-1.6		-1.5
HVO_2544	<i>rpsS</i>	30S ribosomal protein S5	0			GIP	TL			-1.6		ns
HVO_0790	<i>fba2</i>	2-amino-3,7-dideoxy-D-threo-hept-6-ulosonate synthase	0			MET	AA			-1.6		ns
HVO_1751	<i>copA</i>	<b>P-type transport ATPase (probable substrate copper/metal cation)</b>	8			TP_CP	TP			-1.7		-1.7
HVO_0841	<i>petD</i>	<b>Cytochrome bc1 complex Cytochrome b/c subunit</b>	5			MET	EM			-1.7		ns
HVO_0773		Probable S-adenosylmethionine-dependent methyltransferase	0			MIS	GEN			-1.7		ns
HVO_2398	<i>znuC1</i>	ABC-type transport system ATP-binding protein (probable substrate zinc)	0			TP_CP	TP			-1.7		-1.6
HVO_1478	<i>ffbS</i>	Transcription initiation factor TFB	0			GIP	TC			-1.8		ns
HVO_B0134		ABC-type transport system ATP-binding protein	0			TP_CP	TP			-1.8		-1.7
HVO_2554	<i>np14</i>	50S ribosomal protein L14	0			GIP	TL			-1.8		ns
HVO_2981	<i>upp</i>	Uracil phosphoribosyltransferase	0			MET	NUM			-1.9		ns
HVO_1241	<i>prnC</i>	SCO1/SenC/PrnC family protein	0	Tat	yes	MIS	GEN			-2.0		-1.5
HVO_0536	<i>dpsA1</i>	Ferritin	0			MIS	MIS			-2.2		ns
HVO_0727		<b>Rhomboid protease II</b>	6			MIS	GEN			-6.6		-6.7
HVO_1274		<b>Conserved hypothetical protein</b>	7			UNASS	CHY			-6.6		-5.5
HVO_1532		<b>DUF368 family protein</b>	8			MIS	GEN			-6.6		ns



Table 2. continued

ID	gene name	protein name	TMS	signal peptide	lipobox	FC	SC	fold S1	fold S2	fold S3	fold S4	total fold
HVO_1914	<i>acaB3</i>	Acetyl-CoA C-acyltransferase	0			MET	LIP			-7.4		-5.1
HVO_1936	<i>cofE</i>	F420-0:gamma-glutamyl ligase	0			MET	COM			-7.4		-6.1
HVO_2318	<i>uppS2</i>	Tritrans-polycis-undecaprenyl-diphosphate synthase	0			MET	LIP			-7.5		ns
HVO_2055	<i>agf15</i>	Probable low-salt glycyl biosynthesis flippase Agf15	14			TP_CP	TP			-8.1		ns
HVO_2602		Transport protein (probable substrate zinc/cadmium)	4			TP_CP	TP			-8.4		-6.9
HVO_2952	<i>endA</i>	tRNA-splicing endonuclease	0			GIP	RMT			-8.4		-6.9
HVO_0972	<i>pilA1</i>	Pilin (PilA1)	1			MIS	MIS				11.7	2.0
HVO_2773	<i>rps2</i>	30S ribosomal protein S2 1	0			GIP	TL				10.6	ns
HVO_0531	<i>tsbB1</i>	ABC-type transport system permease protein (probable substrate sugar)	0			TP_CP	TP				8.6	ns
HVO_1110	<i>btuF</i>	ABC-type transport system periplasmic substrate-binding protein (probable substrate cobalamin)	0	Sec		TP_CP	TP				7.1	ns
HVO_2163		ABC-type transport system ATP-binding protein (homologue to LolDCE lipoprotein release factor)	0			TP_CP	TP				7.1	ns
HVO_2547	<i>rpl32e</i>	50S ribosomal protein L32e	0			GIP	TL				1.9	ns
HVO_2564	<i>rpl3</i>	50S ribosomal protein L3	0			GIP	TL				1.7	ns
HVO_0316	<i>atpA</i>	A-type ATP synthase subunit A	0			MET	EM				1.6	ns
HVO_0060	<i>dppC1</i>	ABC-type transport system permease protein (probable substrate dipeptide/oligopeptide)	8			TP_CP	TP				-1.5	ns
HVO_B0185	<i>dppB14</i>	ABC-type transport system permease protein (probable substrate dipeptide/oligopeptide)	6			TP_CP	TP				-1.6	ns
HVO_0500		Conserved hypothetical protein	1			UNASS	CHY				-1.6	ns
HVO_1198		UspA domain protein	0			MIS	GEN				-1.8	ns
HVO_0146	<i>psd</i>	Phosphatidylserine decarboxylase	1			MET	LIP				-2.5	ns
HVO_1563		Conserved hypothetical protein	0	Sec		UNASS	CHY				-2.6	-1.6
HVO_1377		UPF0145 family protein	0			MIS	GEN				-13.4	-6.9

“Membrane protein samples (triplicates) from exponentially growing MIG1 and wt cells were subjected to SDS-PAGE allowed to run for 2 cm and separated in four sections (top to bottom: S1–S4), which were analyzed separately by RPLC–MS/MS, as indicated in Table 1. Regulation factors were submitted to a Student’s *t*-test, and proteins with *p*-values  $\leq 0.05$  and fold  $\geq 1.5$  were considered significant. In bold, integral membrane proteins; ns, not significant.

Several proteins involved in solute transport across cell membranes showed altered electrophoretic migration including 16 ABC transporter components for lipoproteins, peptides,  $\text{Zn}^{2+}$ , cobalamin, phosphate, and sugars (Table 2). In addition, three integral membrane metal transporters (probable Zn/Cd transport protein-HVO\_2602 and P-type ATPase-HVO\_1751, Mg transport protein CorA-HVO\_1675) displayed altered migration with negative folds of 8.4 (section 3), 1.7 (section 3) and 5.2 (section 2), respectively. P-type ATPase also showed reduced levels in quantitative proteomics experiment (see previous). It is possible that differences in metal ion availability would in turn cause to some extent variations in other metalloprotein levels (i.e., metalloproteases, see previous). Metal ions have a key role in the physiology of cells, as they act as the redox centers for metalloproteins such as cytochromes, blue copper proteins, and iron–sulfur proteins, which play a vital role in electron transport. On the other hand, any disturbance in metal ion homeostasis could produce toxic effects on cell viability. Among Archaea, thermophiles, hyperthermophiles, and methanogens utilize P-type ATPases and ABC transporters for metal transport and balancing. However, metal homeostasis in haloarchaea has not been extensively studied.<sup>59</sup> Independently, if the observed difference in concentration of metal transporter proteins is a direct or indirect effect of RhoII absence, these data, together with the semiquantitative proteomics results (Table 1), suggest that metal homeostasis is affected in MIG1. However, under standard laboratory conditions, this effect was not reflected in cell proliferation and growth.

### 3.6. Proteins with Differential Migration Related to Phenotypes of the MIG1 Strain

**3.6.1. Soluble Proteins.** DNA gyrase is an essential bacterial enzyme that catalyzes the ATP-dependent negative supercoiling of double-stranded closed circular DNA. Gyrase is a topoisomerase involved in the control of topological transitions of DNA.<sup>60</sup> The active form of this enzyme is a tetramer of two A and two B subunits.<sup>61</sup> Novobiocin is a DNA gyrase inhibitor that binds to the active enzyme.<sup>62</sup> In this work, we observed that the DNA gyrase subunit A was reduced by about two-fold in section 2 of the PROTOMAP gel (Table 2). The abnormal migration of subunit A in the *rhoII* mutant suggests that migration of this polypeptide is altered (i.e., affected by post translational modification) generating a DNA gyrase more susceptible to novobiocin inhibition that could account for the enhanced sensitivity to novobiocin displayed by the MIG1 strain.<sup>17</sup>

In *H. volcanii*, the *rhoII* gene is part of an operon with the sequence encoding EndV (HVO\_0726), an endonuclease involved in DNA repair in *E. coli*.<sup>63</sup> We have shown that *endV* mRNA is expressed in *H. volcanii* H26 and MIG1 at similar levels.<sup>17</sup> MIG1 cells irradiated with UV light in liquid minimal medium cultures, showed a delay in resuming growth when compared to the wt (Figure S2), evidencing that the mutant has difficulty in coping with UV stress. In this study, the soluble protein RadA (HVO\_0104), which is involved in DNA repair after UV irradiation,<sup>64</sup> was reduced by 1.9-fold in section 2 in the mutant (Table 2). Even though the functional link between RhoII, EndV and RadA remains to be addressed, our data suggest that RhoII may participate in the regulation of DNA repair processes in *H. volcanii*. A link between UV irradiation and Rho has been reported for RHBDL2, which

showed upregulation upon UV treatment in human keratinocytes.<sup>65</sup>

**3.6.2. Integral Membrane Proteins.** *H. volcanii* is surrounded by a hexagonally packed surface S-layer, formed by the SLG. This glycoprotein contains seven predicted N-glycosylation sites. Out of these, N83, N13, N274, and N279 are decorated with a pentasaccharide, which also occurs in *H. volcanii* flagellins and pilins.<sup>66–68</sup> In addition, position N498 is decorated with a tetrasaccharide synthesized only in low salt growth conditions.<sup>69</sup> Our previous work showed that N-732 in the SLG harbors a novel sulfoquinovose containing oligosaccharide (GlcNAc–GlcNAc(Hex)<sub>2</sub>–(SQ-Hex)<sub>6</sub>), which is truncated in the MIG1 strain.<sup>17</sup>

Several enzymes potentially involved in protein glycosylation were detected as differential by shotgun proteomics (Table 1) and in the PROTOMAP experiment (Table 2). A list along with their proposed/known roles is provided in Table S2. Agl15 (HVO\_2050), a flippase that participates in the synthesis of low salt tetrasaccharide at position N498 of SLG,<sup>68</sup> was the only affected glycosylase predicted to be an integral membrane protein (14 TMS) with an 8.1-fold reduction at section 3 of the PROTOMAP. Whether this protein is involved in the N-732 glycosylation of SLG is not known. However, if this were the case, Agl15 processing/activation by RhoII may account at least in part for the differences in SLG glycosylation observed in the mutant.<sup>17</sup> Alternatively, it is also possible that RhoII cleaves an unknown substrate that regulates the level of one or more of these glycosylation enzyme/s (Table S2) leading to an abnormal glycosylation pattern of the SLG.

SLG is initially synthesized with a C-terminal transmembrane domain and following proteolytic cleavage upstream of the TMS, the truncated protein is transferred to a lipid anchor.<sup>70</sup> The involvement of the ArtA archaeosortase in the proteolytic processing of the C-terminus of this glycoprotein was reported by Abdul Halim et al.<sup>71</sup> In this study, SLG was enriched 1.5-fold in section 2 and 1.7-fold in section 3 of the PROTOMAP (Table 2). The differential electrophoretic migration of this protein may be due to the previously observed truncation of the oligosaccharide bound to N732 in the mutant strain. However, it cannot be ruled out that RhoII may also contribute to proteolytic processing of SLG.

The preflagellin peptidase PibD was reduced 7.7-fold in section 3 and evidenced a two-fold reduction in level when calculating the total fold (Table 2), indicating that its electrophoretic migration was altered but also that the protein concentration was lower in MIG1 cells. PibD is known to process preflagellins and prepilins prior to flagella and pili assembly in archaea.<sup>72</sup> It was shown that a knockout mutation of *pibD* abolished swimming motility and adhesion to glass surfaces in *H. volcanii*.<sup>33</sup> Therefore, decreased amounts of PibD in MIG1 cells may explain the reduced motility of this strain in soft agar plates.<sup>17</sup> To determine whether cell adhesion was also affected in the MIG1 mutant, we examined the ability of these cells to adhere to glass slides. As observed in Figure 5, the Rho mutant showed reduced adhesion to glass plates compared to the parental strain. In addition, PilA1 (HVO\_0972), a substrate of PibD,<sup>72</sup> was accumulated in section 4 of the gel. It could be proposed that RhoII is involved in proteolytic maturation/processing of PibD affecting pilin (and probably flagellin, see Table 1) processing or assembly and therefore *H. volcanii* motility.

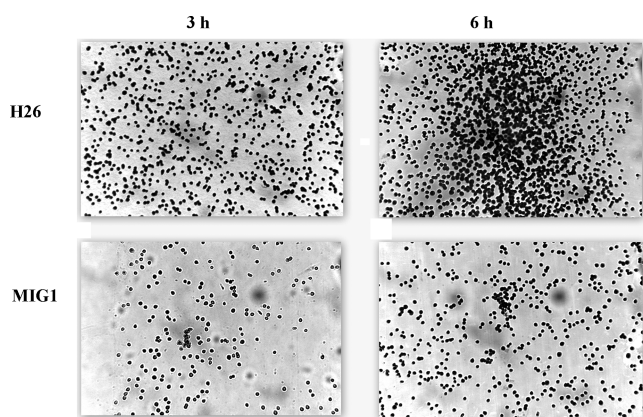


**Figure 5.** Cells from *H. volcanii* MIG1 strain show reduced adhesion to glass surfaces. Adhesion to glass coverslips was tested using a previously described protocol.<sup>33</sup> Coverslips were placed in 50 mL plastic tubes containing 6 mL of MGM 18% medium cultures of *H. volcanii* H26 and MIG1 at an OD<sub>600</sub> of 0.3. After 3 or 6 h incubation at 42 °C, cells were fixed with 2% acetic acid, stained with 0.1% crystal violet, and observed by light microscopy. Light micrographs of the coverslips were taken at 100× magnification.

### 3.7. Analysis of Semitryptic Peptides in Integral Membrane Proteins

Detection of proteins with different levels or electrophoretic mobility variations was performed against a trypsin digestion

database. To identify peptides that may result from RhoII proteolytic activity, a search of semitryptic peptides was also performed. This analysis focused on proteins with semitryptic peptide(s) (found exclusively in the wt) inside or near a TMS and that evidenced a Rho cleavage motif (Table S4). A total of 10 candidates were identified in all the experiments performed including PibD, hypothetical proteins, and small solute transporters. However, it must be noted that it is not known whether archaeal rhomboid proteases recognize the same cleavage motif as their bacterial and eukaryotic counterparts. Experimental validation and cleavage site identification of *H. volcanii* RhoII predicted substrates will contribute to clarify this particular issue.

### 4. CONCLUDING REMARKS

This study shows, for the first time, the effect of a rhomboid protease gene deletion on the proteome of an archaeon. Previous studies have examined the influence of Rho deficiency on specific subproteomes, such as *A. thaliana* chloroplasts<sup>73</sup> and the secretome of *Trichomonas vaginalis*;<sup>74</sup> however, our study focused on a more comprehensive analysis of the relevance of Rho at the whole proteome level.

Elimination of *rhoII* from *H. volcanii* chromosome had a global impact on the proteome, affecting soluble and membrane-associated as well as secreted proteins with diverse biological functions, suggesting a role for this protease in the regulation of processes such as solute transport, Cu homeostasis, signal transduction, protein glycosylation, cell adhesion,

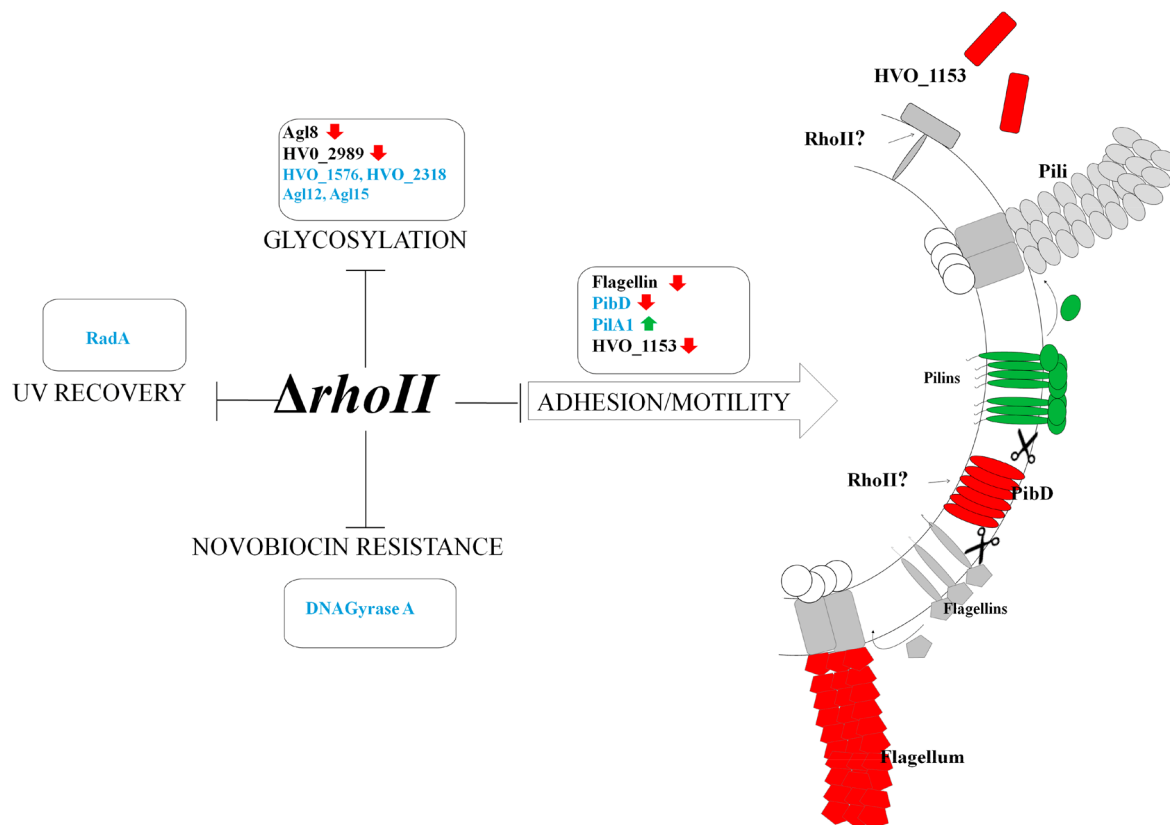


**Figure 6.** Schematic representation of the effect of deleting *rhoII* in *H. volcanii* physiology. Elimination of *rhoII* from the chromosome causes several phenotypes in *H. volcanii* cells. Proteins that showed variations in level or electrophoretic mobility in this work and that are potentially involved in the generation of these phenotypes are listed in the corresponding box. Blue font denotes proteins that showed differential migration in the PROTOMAP assay. The arrows indicate proteins with augmented (green) or decreased concentration (red) in the mutant. The proposed role of RhoII in the processing of the conserved hypothetical protein HVO\_1153 and PibD (affecting cell adhesion and motility) is detailed on the right.



and motility. Interestingly, some of these proteins are associated with the differential phenotypes observed in the *rhoII* mutant. A schematic representation of the proteins showing differences in their levels or electrophoretic migration and their involvement in the generation of the mutant phenotypes is provided in Figure 6. Ongoing work is focused on the validation of selected candidate substrates of RhoII, which will contribute to get insight on the biological function of this family of IMPs in the *Archaea* domain.

## ■ ASSOCIATED CONTENT

### ● Supporting Information

The Supporting Information is available free of charge on the ACS Publications website at DOI: 10.1021/acs.jproteome.7b00530.

Cartoon representation of SDS gels used for comparative quantitative proteomics or simplified PROTOMAP assay sample preparation; effect of UV irradiation on *H. volcanii* MIG1 growth; proteins involved in N-glycosylation with affected level or migration in MIG1; semitryptic peptides with rhomboid cleavage consensus detected in membrane proteins (PDF)

Proteins detected in membrane, cytoplasm, and cell culture supernatants of *H. volcanii* H26 and MIG1 at exp and st phase of growth; proteins detected in membranes of exponentially growing H26 and MIG1 strains in the PROTOMAP assay (XLSX)

## ■ AUTHOR INFORMATION

### Corresponding Authors

\*E-mail: [ansgar.poetsch@rub.de](mailto:ansgar.poetsch@rub.de).

\*E-mail: [migimen@mdp.edu.ar](mailto:migimen@mdp.edu.ar). Phone: 54-223-4753030 int 12.

### ORCID

María I. Giménez: 0000-0002-2188-4154

### Author Contributions

<sup>†</sup>These authors contributed equally to this work.

### Notes

The authors declare no competing financial interest.

## ■ ACKNOWLEDGMENTS

This work was supported by CONICET Grant (PIP-1106), UNMdP Grant EXA632/13. Agencia Nacional de Promoción Científica y Tecnológica (ANPCyT) Grant PICT1477. M.I.C. is an ANPCyT Doctoral Fellow, and M.C. is a CONICET Post-Doctoral Fellow.

## ■ ABBREVIATIONS

Rho, rhomboid proteases; IMP, intramembrane protease; TMS, transmembrane segment; exp, exponential; st, stationary; nLC-ESI-MS/MS, nanoscale liquid chromatographic-electrospray ionization-tandem mass spectrometry; SLG, S-layer glycoprotein

## ■ REFERENCES

- (1) Lopez-Otin, C.; Overall, C. M. Protease degradomics: a new challenge for proteomics. *Nat. Rev. Mol. Cell Biol.* **2002**, *3* (7), 509–19.
- (2) Gimenez, M. I.; Cerletti, M.; De Castro, R. E. Archaeal membrane-associated proteases: insights on *Haloferax volcanii* and other haloarchaea. *Front. Microbiol.* **2015**, *6*, 39.
- (3) Verhelst, S. H. Intramembrane proteases as drug targets. *FEBS J.* **2017**, *284* (10), 1489–1502.
- (4) Freeman, M. The rhomboid-like superfamily: molecular mechanisms and biological roles. *Annu. Rev. Cell Dev. Biol.* **2014**, *30*, 235–54.
- (5) Lee, J. R.; Urban, S.; Garvey, C. F.; Freeman, M. Regulated intracellular ligand transport and proteolysis control EGF signal activation in *Drosophila*. *Cell* **2001**, *107* (2), 161–71.
- (6) Urban, S.; Lee, J. R.; Freeman, M. A family of Rhomboid intramembrane proteases activates all *Drosophila* membrane-tethered EGF ligands. *EMBO journal* **2002**, *21* (16), 4277–86.
- (7) Spinazzi, M.; De Strooper, B. PARL: The mitochondrial rhomboid protease. *Semin. Cell Dev. Biol.* **2016**, *60*, 19–28.
- (8) Sibley, L. D. The roles of intramembrane proteases in protozoan parasites. *Biochim. Biophys. Acta, Biomembr.* **2013**, *1828* (12), 2908–15.
- (9) Dhingra, S.; Kowlaski, C. H.; Thammahong, A.; Beattie, S. R.; Bultman, K. M.; Cramer, R. A. RbdB, a Rhomboid Protease Critical for SREBP Activation and Virulence in *Aspergillus fumigatus*. *mSphere* **2016**, *1* (2), e00035–16.
- (10) Stevenson, L. G.; Strisovsky, K.; Clemmer, K. M.; Bhatt, S.; Freeman, M.; Rather, P. N. Rhomboid protease AarA mediates quorum-sensing in *Providencia stuartii* by activating TATA of the twin-arginine translocase. *Proc. Natl. Acad. Sci. U. S. A.* **2007**, *104* (3), 1003–8.
- (11) Akiyama, Y.; Maegawa, S. Sequence features of substrates required for cleavage by GlpG, an *Escherichia coli* rhomboid protease. *Mol. Microbiol.* **2007**, *64* (4), 1028–37.
- (12) Maegawa, S.; Ito, K.; Akiyama, Y. Proteolytic action of GlpG, a rhomboid protease in the *Escherichia coli* cytoplasmic membrane. *Biochemistry* **2005**, *44* (41), 13543–52.
- (13) Erez, E.; Bibi, E. Cleavage of a multispanning membrane protein by an intramembrane serine protease. *Biochemistry* **2009**, *48* (51), 12314–22.
- (14) Mesak, L. R.; Mesak, F. M.; Dahl, M. K. Expression of a novel gene, *glpP*, is essential for normal *Bacillus subtilis* cell division and contributes to glucose export. *BMC Microbiol.* **2004**, *4*, 13.
- (15) Kateete, D. P.; Katabazi, F. A.; Okeng, A.; Okee, M.; Musinguzi, C.; Asiimwe, B. B.; Kyobe, S.; Asiimwe, J.; Boom, W. H.; Joloba, M. L. Rhomboids of *Mycobacteria*: characterization using an *aarA* mutant of *Providencia stuartii* and gene deletion in *Mycobacterium smegmatis*. *PLoS One* **2012**, *7* (9), e45741.
- (16) Kinch, L. N.; Grishin, N. V. Bioinformatics perspective on rhomboid intramembrane protease evolution and function. *Biochim. Biophys. Acta, Biomembr.* **2013**, *1828* (12), 2937–43.
- (17) Parente, J.; Casabuono, A.; Ferrari, M. C.; Paggi, R. A.; De Castro, R. E.; Couto, A. S.; Giménez, M. I. A rhomboid protease gene deletion affects a novel oligosaccharide N-linked to the S-layer glycoprotein of *Haloferax volcanii*. *J. Biol. Chem.* **2014**, *289* (16), 11304–17.
- (18) Cerletti, M.; Paggi, R. A.; Guevara, C. R.; Poetsch, A.; De Castro, R. E. Global role of the membrane protease LonB in *Archaea*: Potential protease targets revealed by quantitative proteome analysis of a *lonB* mutant in *Haloferax volcanii*. *J. Proteomics* **2015**, *121*, 1–14.
- (19) Nieuwlandt, D. T.; Palmer, J. R.; Armbruster, D. T.; Kuo, Y. P.; Oda, W.; Daniels, C. J. *Archaea: A Laboratory Manual*; Robb, F. T., Place, A. R., Sowers, K. R., Schreier, H. J., DasSarma, S., Fleischmann, E. M., Eds.; Cold Spring Harbor Laboratory Press: Cold Spring Harbor, NY, 1995; pp 161–162.
- (20) Dyall-Smith, M. The halo handbook. *Protocols for Haloarchaeal Genetics*; Dyall-Smith, M.; University of Melbourne, 2009; p 144. <http://www.haloarchaea.com/resources/halohandbook/>.
- (21) Sambrook, J.; Russell, D. W. *Molecular Cloning: A Laboratory Manual*; Cold Spring Harbor Laboratory Press: Cold Spring Harbor, NY, 2001.
- (22) Laemmli, U. K. Cleavage of structural proteins during the assembly of the head of bacteriophage T4. *Nature* **1970**, *227* (5259), 680–5.

- (23) Dix, M. M.; Simon, G. M.; Cravatt, B. F. Global identification of caspase substrates using PROTOPAP (protein topography and migration analysis platform). *Methods Mol. Biol.* **2014**, *1133*, 61–70.
- (24) Candiano, G.; Bruschi, M.; Musante, L.; Santucci, L.; Ghiggeri, G. M.; Carnemolla, B.; Orecchia, P.; Zardi, L.; Righetti, P. G. Blue silver: a very sensitive colloidal Coomassie G-250 staining for proteome analysis. *Electrophoresis* **2004**, *25* (9), 1327–33.
- (25) Schluesener, D.; Fischer, F.; Kruij, J.; Rogner, M.; Poetsch, A. Mapping the membrane proteome of *Corynebacterium glutamicum*. *Proteomics* **2005**, *5* (5), 1317–30.
- (26) Eng, J. K.; McCormack, A. L.; Yates, J. R. An approach to correlate tandem mass spectral data of peptides with amino acid sequences in a protein database. *J. Am. Soc. Mass Spectrom.* **1994**, *5* (11), 976–989.
- (27) Dorfer, V.; Pichler, P.; Stranzl, T.; Stadlmann, J.; Taus, T.; Winkler, S.; Mechtler, K. MS Amanda, a universal identification algorithm optimized for high accuracy tandem mass spectra. *J. Proteome Res.* **2014**, *13* (8), 3679–84.
- (28) Pfeiffer, F.; Broicher, A.; Gillich, T.; Klee, K.; Mejia, J.; Rampp, M.; Oesterhelt, D. Genome information management and integrated data analysis with HaloLex. *Arch. Microbiol.* **2008**, *190* (3), 281–99.
- (29) Kall, L.; Storey, J. D.; MacCoss, M. J.; Noble, W. S. Posterior error probabilities and false discovery rates: two sides of the same coin. *J. Proteome Res.* **2008**, *7* (1), 40–4.
- (30) Liu, H.; Sadygov, R. G.; Yates, J. R., 3rd A model for random sampling and estimation of relative protein abundance in shotgun proteomics. *Anal. Chem.* **2004**, *76* (14), 4193–201.
- (31) Haussmann, U.; Qi, S. W.; Wolters, D.; Rogner, M.; Liu, S. J.; Poetsch, A. Physiological adaptation of *Corynebacterium glutamicum* to benzoate as alternative carbon source - a membrane proteome-centric view. *Proteomics* **2009**, *9* (14), 3635–51.
- (32) Allers, T.; Barak, S.; Liddell, S.; Wardell, K.; Mevarech, M. Improved strains and plasmid vectors for conditional overexpression of His-tagged proteins in *Haloferax volcanii*. *Applied and environmental microbiology* **2010**, *76* (6), 1759–69.
- (33) Tripepi, M.; Imam, S.; Pohlschroder, M. *Haloferax volcanii* flagella are required for motility but are not involved in PibD-dependent surface adhesion. *Journal of bacteriology* **2010**, *192* (12), 3093–102.
- (34) Fischer, F.; Poetsch, A. Protein cleavage strategies for an improved analysis of the membrane proteome. *Proteome Sci.* **2006**, *4*, 2.
- (35) Heberle, H.; Meirles, G. V.; da Silva, F. R.; Telles, G. P.; Minghim, R. InteractiVenn: a web-based tool for the analysis of sets through Venn diagrams. *BMC Bioinf.* **2015**, *16*, 169.
- (36) Stuart, J. A.; Mayard, S.; Hashiguchi, K.; Souza-Pinto, N. C.; Bohr, V. A. Localization of mitochondrial DNA base excision repair to an inner membrane-associated particulate fraction. *Nucleic Acids Res.* **2005**, *33* (12), 3722–32.
- (37) Tsruya, R.; Wojtalla, A.; Carmon, S.; Yogeve, S.; Reich, A.; Bibi, E.; Merdes, G.; Schejter, E.; Shilo, B. Z. Rhomboid cleaves Star to regulate the levels of secreted Spitz. *EMBO J.* **2007**, *26* (5), 1211–20.
- (38) Strisovsky, K. Structural and mechanistic principles of intramembrane proteolysis—lessons from rhomboids. *FEBS J.* **2013**, *280* (7), 1579–603.
- (39) Strisovsky, K.; Sharpe, H. J.; Freeman, M. Sequence-specific intramembrane proteolysis: identification of a recognition motif in rhomboid substrates. *Mol. Cell* **2009**, *36* (6), 1048–59.
- (40) Scharf, B.; Engelhard, M. Halocyanin, an archaeobacterial blue copper protein (type I) from *Natronobacterium pharaonis*. *Biochemistry* **1993**, *32* (47), 12894–900.
- (41) Zhang, L.; McSpadden, B.; Pakrasi, H. B.; Whitmarsh, J. Copper-mediated regulation of cytochrome c553 and plastocyanin in the cyanobacterium *Synechocystis* 6803. *J. Biol. Chem.* **1992**, *267* (27), 19054–9.
- (42) Kropat, J.; Gallaher, S. D.; Urzica, E. I.; Nakamoto, S. S.; Strenkert, D.; Tottey, S.; Mason, A. Z.; Merchant, S. S. Copper economy in *Chlamydomonas*: prioritized allocation and reallocation of copper to respiration vs. photosynthesis. *Proc. Natl. Acad. Sci. U. S. A.* **2015**, *112* (9), 2644–51.
- (43) Abdel-Ghany, S. E.; Pilon, M. MicroRNA-mediated systemic down-regulation of copper protein expression in response to low copper availability in *Arabidopsis*. *J. Biol. Chem.* **2008**, *283* (23), 15932–45.
- (44) Mattar, S.; Scharf, B.; Kent, S. B.; Rodewald, K.; Oesterhelt, D.; Engelhard, M. The primary structure of halocyanin, an archaeal blue copper protein, predicts a lipid anchor for membrane fixation. *J. Biol. Chem.* **1994**, *269* (21), 14939–45.
- (45) Shikanai, T.; Muller-Moule, P.; Munekage, Y.; Niyogi, K. K.; Pilon, M. PAA1, a P-type ATPase of *Arabidopsis*, functions in copper transport in chloroplasts. *Plant Cell* **2003**, *15* (6), 1333–46.
- (46) Abdel-Ghany, S. E.; Muller-Moule, P.; Niyogi, K. K.; Pilon, M.; Shikanai, T. Two P-type ATPases are required for copper delivery in *Arabidopsis thaliana* chloroplasts. *Plant Cell* **2005**, *17* (4), 1233–51.
- (47) Migocka, M. Copper-transporting ATPases: The evolutionarily conserved machineries for balancing copper in living systems. *IUBMB Life* **2015**, *67* (10), 737–45.
- (48) Arguello, J. M. Identification of ion-selectivity determinants in heavy-metal transport P1B-type ATPases. *J. Membr. Biol.* **2003**, *195* (2), 93–108.
- (49) Völlmecke, C.; Drees, S. L.; Reimann, J.; Albers, S.-V.; Lübbers, M. The ATPases CopA and CopB both contribute to copper resistance of the thermoacidophilic archaeon *Sulfolobus solfataricus*. *Microbiology* **2012**, *158* (6), 1622–1633.
- (50) Wan, C.; Fu, J.; Wang, Y.; Miao, S.; Song, W.; Wang, L. Exosome-related multi-pass transmembrane protein TSAP6 is a target of rhomboid protease RHBDD1-induced proteolysis. *PLoS One* **2012**, *7* (5), e37452.
- (51) Wai, T.; Saita, S.; Nolte, H.; Muller, S.; König, T.; Richter-Dennerlein, R.; Sprenger, H. G.; Madrenas, J.; Muhlmeister, M.; Brandt, U.; Krüger, M.; Langer, T. The membrane scaffold SLP2 anchors a proteolytic hub in mitochondria containing PARL and the i-AAA protease YME1L. *EMBO Rep.* **2016**, *17* (12), 1844–1856.
- (52) Heinrich, J.; Hein, K.; Wiegert, T. Two proteolytic modules are involved in regulated intramembrane proteolysis of *Bacillus subtilis* RsiW. *Mol. Microbiol.* **2009**, *74* (6), 1412–26.
- (53) Ellen, A. F.; Zolghadr, B.; Driessen, A. M.; Albers, S.-V. Shaping the archaeal cell envelope. *Archaea* **2010**, *2010*, 13.
- (54) Feng, J.; Wang, J.; Zhang, Y.; Du, X.; Xu, Z.; Wu, Y.; Tang, W.; Li, M.; Tang, B.; Tang, X. F. Proteomic analysis of the secretome of haloarchaeon *Natrinema* sp. J7–2. *J. Proteome Res.* **2014**, *13* (3), 1248–58.
- (55) Hand, N. J.; Klein, R.; Laskewitz, A.; Pohlschroder, M. Archaeal and bacterial SecD and SecF homologs exhibit striking structural and functional conservation. *Journal of bacteriology* **2006**, *188* (4), 1251–9.
- (56) Fink-Lavi, E.; Eichler, J. Identification of residues essential for the catalytic activity of Sec11b, one of the two type I signal peptidases of *Haloferax volcanii*. *FEMS Microbiol. Lett.* **2008**, *278* (2), 257–60.
- (57) Gupta, R.; Brunak, S. Prediction of glycosylation across the human proteome and the correlation to protein function. *Pacific Symposium on Biocomputing. Pacific Symposium on Biocomputing* **2002**, 310–22.
- (58) Urban, S.; Dickey, S. W. The rhomboid protease family: a decade of progress on function and mechanism. *Genome biology* **2011**, *12* (10), 231.
- (59) Srivastava, P.; Kowshik, M. Mechanisms of metal resistance and homeostasis in haloarchaea. *Archaea* **2013**, *2013*, 732864.
- (60) Reece, R. J.; Maxwell, A. DNA gyrase: structure and function. *Crit. Rev. Biochem. Mol. Biol.* **1991**, *26* (3–4), 335–75.
- (61) Maxwell, A.; Bush, N. G.; Evans-Roberts, K. DNA Topoisomerases. *EcoSal Plus* **2015**, DOI: 10.1128/ecosalplus.ESP-0010-2014.
- (62) Heide, L. New aminocoumarin antibiotics as gyrase inhibitors. *Int. J. Med. Microbiol.* **2014**, *304* (1), 31–6.
- (63) Kuraoka, I. Diversity of Endonuclease V: From DNA Repair to RNA Editing. *Biomolecules* **2015**, *5* (4), 2194–206.
- (64) Woods, W. G.; Dyall-Smith, M. L. Construction and analysis of a recombination-deficient (radA) mutant of *Haloferax volcanii*. *Mol. Microbiol.* **1997**, *23* (4), 791–7.

- (65) Cheng, T. L.; Wu, Y. T.; Lin, H. Y.; Hsu, F. C.; Liu, S. K.; Chang, B. I.; Chen, W. S.; Lai, C. H.; Shi, G. Y.; Wu, H. L. Functions of rhomboid family protease RHBDL2 and thrombomodulin in wound healing. *J. Invest. Dermatol.* **2011**, *131* (12), 2486–94.
- (66) Kandiba, L.; Lin, C. W.; Aebi, M.; Eichler, J.; Guerardel, Y. Structural characterization of the N-linked pentasaccharide decorating glycoproteins of the halophilic archaeon *Haloferax volcanii*. *Glycobiology* **2016**, *26* (7), 745–56.
- (67) Tripepi, M.; You, J.; Temel, S.; Onder, O.; Brisson, D.; Pohlschroder, M. N-glycosylation of *Haloferax volcanii* flagellins requires known Agl proteins and is essential for biosynthesis of stable flagella. *Journal of bacteriology* **2012**, *194* (18), 4876–87.
- (68) Esquivel, R. N.; Schulze, S.; Xu, R.; Hippler, M.; Pohlschroder, M. Identification of *Haloferax volcanii* Pilin N-Glycans with Diverse Roles in Pilus Biosynthesis, Adhesion, and Microcolony Formation. *J. Biol. Chem.* **2016**, *291* (20), 10602–14.
- (69) Kaminski, L.; Guan, Z.; Yurist-Doutsch, S.; Eichler, J. Two distinct N-glycosylation pathways process the *Haloferax volcanii* S-layer glycoprotein upon changes in environmental salinity. *mBio* **2013**, *4* (6), e00716–13.
- (70) Kandiba, L.; Guan, Z.; Eichler, J. Lipid modification gives rise to two distinct *Haloferax volcanii* S-layer glycoprotein populations. *Biochim. Biophys. Acta, Biomembr.* **2013**, *1828* (3), 938–43.
- (71) Abdul Halim, M. F.; Pfeiffer, F.; Zou, J.; Frisch, A.; Haft, D.; Wu, S.; Tolic, N.; Brewer, H.; Payne, S. H.; Pasa-Tolic, L.; Pohlschroder, M. *Haloferax volcanii* archaeosortase is required for motility, mating, and C-terminal processing of the S-layer glycoprotein. *Mol. Microbiol.* **2013**, *88* (6), 1164–75.
- (72) Esquivel, R. N.; Xu, R.; Pohlschroder, M. Novel archaeal adhesion pilins with a conserved N terminus. *Journal of bacteriology* **2013**, *195* (17), 3808–18.
- (73) Knopf, R. R.; Feder, A.; Mayer, K.; Lin, A.; Rozenberg, M.; Schaller, A.; Adam, Z. Rhomboid proteins in the chloroplast envelope affect the level of allene oxide synthase in *Arabidopsis thaliana*. *Plant J.* **2012**, *72* (4), 559–71.
- (74) Riestra, A. M.; Gandhi, S.; Sweredoski, M. J.; Moradian, A.; Hess, S.; Urban, S.; Johnson, P. J. A *Trichomonas vaginalis* Rhomboid Protease and Its Substrate Modulate Parasite Attachment and Cytolysis of Host Cells. *PLoS Pathog.* **2015**, *11* (12), e1005294.